Elsevier Editorial System(tm) for Wear
Manuscript Draft

Manuscript Number:

Title: Effect of roughness on the wear behavior of HVOF coatings dry sliding against a friction material

Article Type: Full-Length Article

Keywords: dry sliding; HVOF coatings; friction materials; roughness

Corresponding Author: Prof. Giovanni Straffelini, Full professor

Corresponding Author's Institution: Universitá di Trento

First Author: Giovanni Straffelini, Full professor

Order of Authors: Giovanni Straffelini, Full professor; Matteo Federici, Ph.D. student; Cinzia Menapace, Senior Researcher; Alessandro Moscatelli; Stefano Gialanella, Professor

Abstract: WC-CoCr coatings on cast iron discs were prepared with different surface roughness and submitted to dry sliding wear tests against a commercial friction material using a pin-on-disc configuration. The effect of roughness on the friction and wear of tribological system was evaluated. The pin wear rate increases with the coating roughness and becomes very high for roughness values in excess of 1 μm. In contrast, the friction coefficient was found to increase as roughness decreased. The discs wear was anyway negligible. The experimental results were explained considering the characteristics of the friction layer that forms during sliding at the interface of the mating bodies in dependence of the initial roughness of the coatings. It is shown that friction layer plays an important role in determining the relative contribution of the abrasive and adhesive interactions and, thereby, the resulting friction and wear behavior of the tribological system.

WEAR

Confirmation of Authorship

Please save a copy of this MS Word file, complete and upload as the "Confirmation of Authorship" file.

As corresponding author, I Giovanni Straffelini, hereby confirm on behalf of all authors that:

1) The authors have obtained the necessary authority for publication.
2) The paper has not been published previously, that it is not under consideration for publication elsewhere, and that if accepted it will not be published elsewhere in the same form, in English or in any other language, without the written consent of the publisher.
3) The paper does not contain material which has been published previously, by the current authors or by others, of which the source is not explicitly cited in the paper.

Upon acceptance of an article by the journal, the author(s) will be asked to transfer the copyright of the article to the publisher. This transfer will ensure the widest possible dissemination of information.

Novelty Statement

Dear Editor

The present research has been carried out within the REBRAKE project, which is funded by the European Union's Seventh Framework Programme (FP7-PEOPLE-2012-IAPP) and is aimed at developing new friction materials and discs with reduced environmental impact.

Most experimental investigations on the reduction of the wear in braking systems have been especially focused on the optimization of the friction materials, by selecting suitable ingredients and relevant concentrations. The present research is focused instead on reducing the disc wear by thermal spray (conventional WC-Co sprayed by HVOF) that is know to reduce sliding wear in tribological system.

The role of the coating surface roughness has been investigated and the results have been explained making specific reference to the acting wear mechanisms and the corresponding characteristics of the friction layer building up between the pin-disc mating surface during the tests. Special emphasis has been reserved to the charactererization of the friction layer that is known to play an important role in the tribological system under study.

The experimental set up has not been designed with the intention the real brake system action, for which specific equipment, like dyno tests, are available and will possibly used in the future to optimize all the engineering requirements of a real braking system.

Best regards
Prof. Giovanni Straffelini
University of Trento

Effect of roughness on the wear behavior of HVOF coatings dry sliding against a friction material

Matteo Federici[a], Cinzia Menapace[a], Alessandro Moscatelli[b], Stefano Gialanella[a], Giovanni Straffelini[a,*]

[a] Dept. of Industrial Engineering, University of Trento, Via Sommarive 9, Povo, Trento, Italy

[b] Flame Spray, via Leonardo da Vinci 1, Roncello, (MB), Italy

* Correspoding Author

ABSTRACT

WC-CoCr coatings on cast iron discs were prepared with different surface roughness and submitted to dry sliding wear tests against a commercial friction material using a pin-on-disc configuration. The effect of roughness on the friction and wear of tribological system was evaluated. The pin wear rate increases with the coating roughness and becomes very high for roughness values in excess of 1 μm. In contrast, the friction coefficient was found to increase as roughness decreased. The discs wear was anyway negligible. The experimental results were explained considering the characteristics of the friction layer that forms during sliding at the interface of the mating bodies in dependence of the initial roughness of the coatings. It is shown that friction layer plays an important role in determining the relative contribution of the abrasive and adhesive interactions and, thereby, the resulting friction and wear behavior of the tribological system.

Keywords:

Dry sliding; HVOF coatings; friction materials; roughness.

1. Introduction

Recent investigations have shown that the wear fragments produced by the braking systems greatly contribute to the overall emission of particulate matter (PM) in the environment [1-3]. Therefore, a number of investigations have been aimed at understanding the wear mechanisms in the braking pad-disc system to develop guidelines for reducing the emissions [4-7]. The brake pads are usually made of friction material that typically contain a large number of different constituents, including metallic fibers and powder, minerals, ceramic particles, solid lubricants and a phenolic resin that after curing bound all the ingredients together [8, 9]. The disc is usually made of a pearlitic cast iron, although other materials, like stainless steel, Al alloys, composite systems are used for specific applications. Since wear of the cast iron disc contributes by approximately 50% to the whole system wear, important efforts have been initiated to reduce such a contribution. In a previous paper, promising results were obtained using conventional heat-treatments of the cast iron disc [10]. It was demonstrated that wear rates of both disc and adopted friction materials in pin-on-disc wear tests were reduced by almost one order of magnitude.

WC-Co-based coatings obtained by thermal spray are widely used in mechanical applications where a high resistance to sliding wear is required [11-13]. In particular, high velocity oxy-fuel (HVOF) thermal spraying is regarded as one of the best methods for depositing conventional WC-Co feedstock powders [14-15], in view of the good combination of higher deposition rate and lower temperature with respect to plasma deposition. These conditions determine a lower porosity and, therefore, a better wear resistance of the coatings [13-15]. The HVOF WC-Co-based coatings in the as-sprayed condition normally display a hardness in the range 1100-1200 HV, and a surface average roughness, R_a, around 5 μm, depending on the powder particles size and morphology and on the specific spraying parameters [16-21]. Depending on the application, the coatings can be submitted to subsequent grinding in order to reduce the roughness, typically down to 0.1-1 μm range. In the proper conditions, the dry sliding specific wear rates of HVOF WC-Co coatings against steel or a counterface of the same type are approximately in the range 10^{-15} (or less) – 10^{-14} m^2/N, i.e., typical of very mild wear [12, 22]. For these systems, the identified wear mechanisms were: coating delamination, fracture of the carbides, cracking in the metallic phase with following disruption of the carbide-binder interfaces, micro-cutting, extrusion of the binder phase [23]. With regard to the coating microstructure, a quite important role is played by the metal content, and the size and quality of the WC particles [24-28]. In addition, the final properties can be tuned also by changing the type of carbides (using, for example, Cr_3C_2, VC, or mixtures [29-31]), and the type of metallic binder (such as Cr, Ni, or different metals together [11, 13, 32]).

As concerns brake systems, to the Author's knowledge, thermal coatings have been investigated so far mainly in case of train brake discs, where the contact temperature can be very high because of the large frictional heating [33]. In the present paper, the results of an exploratory research aimed at obtaining starting information on the feasibility of thermal spray coatings in the pad-disc braking system for the automotive market are reported, with particular reference to the reduction of PM emissions. The investigation was carried out using a laboratory pin-on-disc testing device, and the tests are thus not meant to reproduce real braking conditions but have the aim of providing preliminary information on the acting wear mechanisms, with particular emphasis to the characteristics of the friction layer, which typically forms at the pin (pad)-disc interface during sliding [34-37]. The pins and discs where machined from commercial brake pads and discs respectively. Each disc was successively coated with a commercial WC-based layer, by an industrial apparatus, using well established operating conditions. Since the hardness of the friction material is typically much lower than that of the cermet coating, a specific attention has been paid to the role of the coating surface

roughness. With this in mind, in the present research the coating roughness was reduced to three different levels in addition to the as-sprayed condition. The resulting wear behavior of the tribological coupling has been evaluated and explained making specific reference to the acting wear mechanisms and the corresponding characteristics of the friction layer building up between the pin-disc mating surface during the tests.

2. Experimental procedure

The discs for the pin-on-disc (PoD) testing had a diameter of 63 mm and were machined from a commercial cast iron disc with a pearlitic microstructure. Successively they were coated on both sides by using an industrial HVOF system and employing a commercial WC-CoCr powder, containing 86%wt. WC particles (with a size in the range 1-10 μm) embedded in a matrix constituted by 10%wt. of Co and 4%wt. of Cr. The feedstock composite powder was produced by agglomeration and sintering and had spherical grains with an average size in the range 15-45 μm. The spray parameters were optimized in previous researchers, and were quite typical for this kind of coating [38, 39]. The kerosene oxygen flow rates, and the spray distance were around 24 L/h, 950 L/min. and 380 mm respectively.

As expected, the surface average roughness, R_a, in the as-sprayed condition was quite high, approximately 5 μm, as measured with a stylus profilometer. Different grinding and polishing procedures were thus adopted to obtain discs with a surface roughness varying in a wide range: from 5μm down to 0.04 μm. Such procedures, carried out using an automatic polishing machine, are described in Table 1, together with the relevant R_a-values. The coatings were observed in a scanning electron microscope (SEM) to reveal the main characteristics of the cross section as well as of the surface topography. Information on the phase composition of the coating was also obtained by means of X-ray diffraction (XRD) measurements, carried out using a Cu-kα radiation.

Table 1. Surface finish of the coated discs.

Final roughness R_a (μm)	Surface finish
5	As sprayed
1	Diamond disc (220 grit) – 30 s
0.1	Diamond disc (220 grit) – 2 min.
0.04	Diamond disc (220 grit) – 2 min. Diamond disc (1200 grit) – 5 min. Cloth + 9 μm diamond paste – 15 min. Cloth + 6 μm diamond paste – 15 min. Cloth + 3 μm diamond paste – 15 min.

Dry sliding tests were carried out using a PoD testing device. The pin (with a diameter 6 mm) was machined from a commercial brake pad made of a low-metallic friction material, with a number of components, the main ones being: zirconia oxide (31 wt-%), Al and Mg silicates (9.5 wt.%), copper and steel fibers (7.5 and 8%), vermiculite (6 wt.%), barite (5 wt.%) and other ingredients, embedded into a phenolic resin matrix. Further details on the characteristics of the adopted friction material can be found in [5] and [40].

The tests were carried out at room temperature at a sliding velocity of 1.57 m/s for 50 min. after a running in step of 10 min. The nominal contact pressure applied was 1 MPa. Pin wear was measured by evaluating the weight loss using an analytical balance with a precision of 10^{-4} g. Wear volumes were determined by dividing the weight loss with the density of the pin (2.9 g/cm^3). The specific wear coefficient, K_a, was calculated using the following expression:

$$Ka = \frac{V}{s\ F_N}$$

where V is the measured wear volume, s is the sliding distance and F_N is the applied load (units: m^2/N).

During the test the friction coefficient was continuously recorded. The evolution of the pin temperature was also monitored through two thermocouples inserted in the pin at a distance of 4 and 6 mm from the contact surface. Worn pins and discs were examined through optical and SEM.

3. Results

3.1 Coatings

Fig. 1 shows a typical cross section of a WC-CoCr coating. The thickness is around 50 μm and the microhardness is 1100 $HV_{0.1}$ approx. The picture at high magnification (Fig. 1b) shows that the coating microstructure is quite typical for this kind of coatings deposited by HVOF using standard parameters [41]. XRD analysis on the coating indicates the presence of about 9% of W_2C, which forms as a consequence of WC decarburization [41, 42].

The surfaces of the coated discs after the different grinding/polishing preparation are shown in figure 2 (a-d). The white areas in Fig. 2b, 2c and 2d represent the grinded/polished parts of the surfaces, i.e., the areas where the highest coating asperities were partially removed by the grinding/polishing action, as schematized in Fig. 2e. The grey areas are the un-polished disc areas, and the black points are pores, which formed during the deposition process.

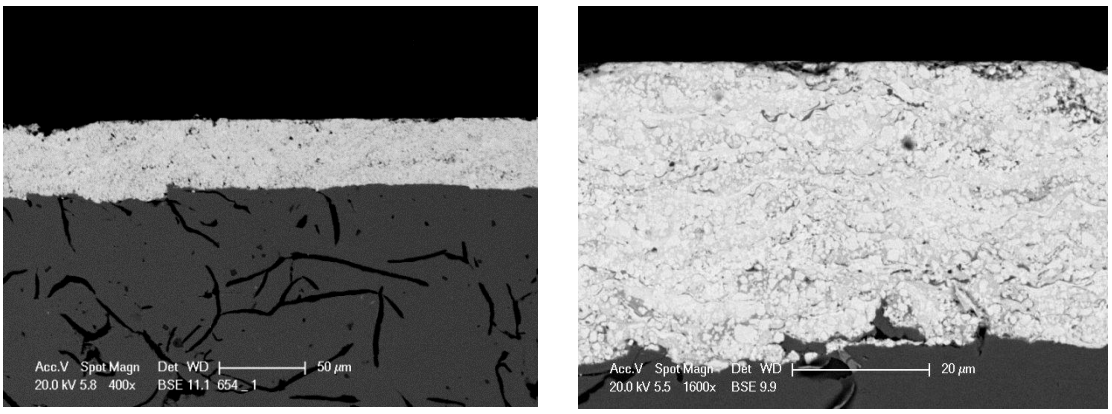

(a) (b)

Fig. 1. Example of cross section of a cast iron disc coated with a WC-CoCr layer. (a) Low magnification; (b) high magnification.

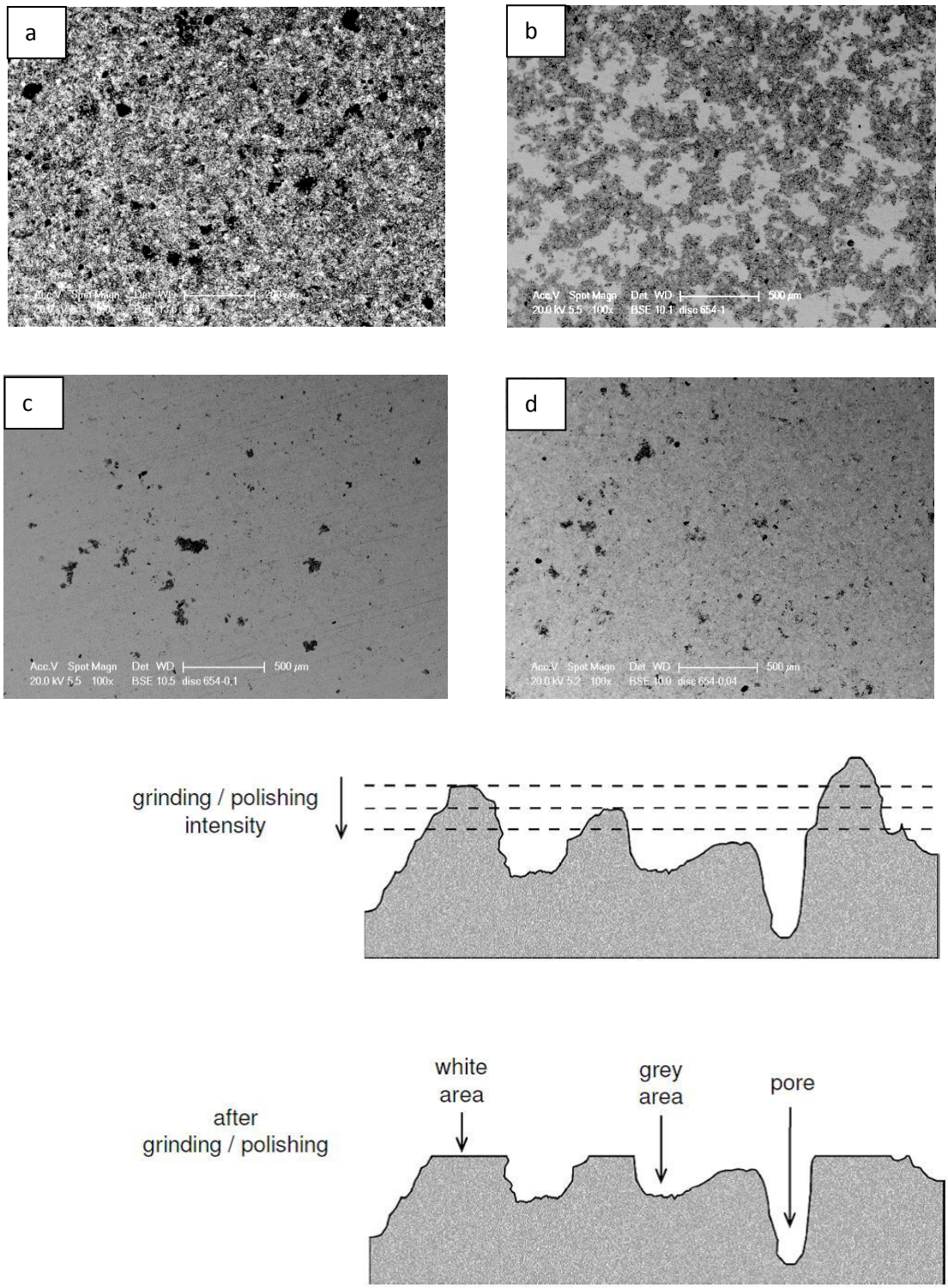

(e)

Fig. 2. Initial disc surfaces. (a) R_a=5 µm, (b) R_a=1 µm, (c) R_a=0.1 µm, (d) R_a=0.04 µm, (e) schematic of the effect of grinding/polishing.

3.2 Friction and wear behavior

In Fig. 3 the friction coefficients recorded during the entire PoD tests in case of the coatings with R_a between 1 and 0.04 μm are displayed. The test on the as-sprayed disc was stopped just after 50 seconds due to the excessive wear, and therefore its friction curve is not displayed herewith. In Fig. 3(d) the temperatures profile recorded during the test against the disc with R_a=0.04 is shown as an example. As already observed in similar tests [43], all the temperatures increase of just a few degrees during the PoD test, in agreement with the fact that most frictional heat flows into the counterface disk and not towards the disk [9, 33, 43, 44].

The friction records show that in all cases the coefficient of friction increases in the first minutes of test (run-in) reaching quite soon a steady value. It is worth noting that the friction trace is less scattered as the coating roughness is decreased. The experimental steady state values of the friction coefficient are listed in Table 2, where all the wear test results are also included (wear volume, wear rate, specific wear coefficient). The friction coefficient increases by decreasing the coating roughness, whereas the wear intensity decreases by decreasing the surface roughness, whereas wear displays a decreasing trend with disc surface roughness. It can be further noted that wear is mild in the case of the coatings with roughness in the range 1-0.04 μm, whereas it is very severe in the case of the as-sprayed coating condition.

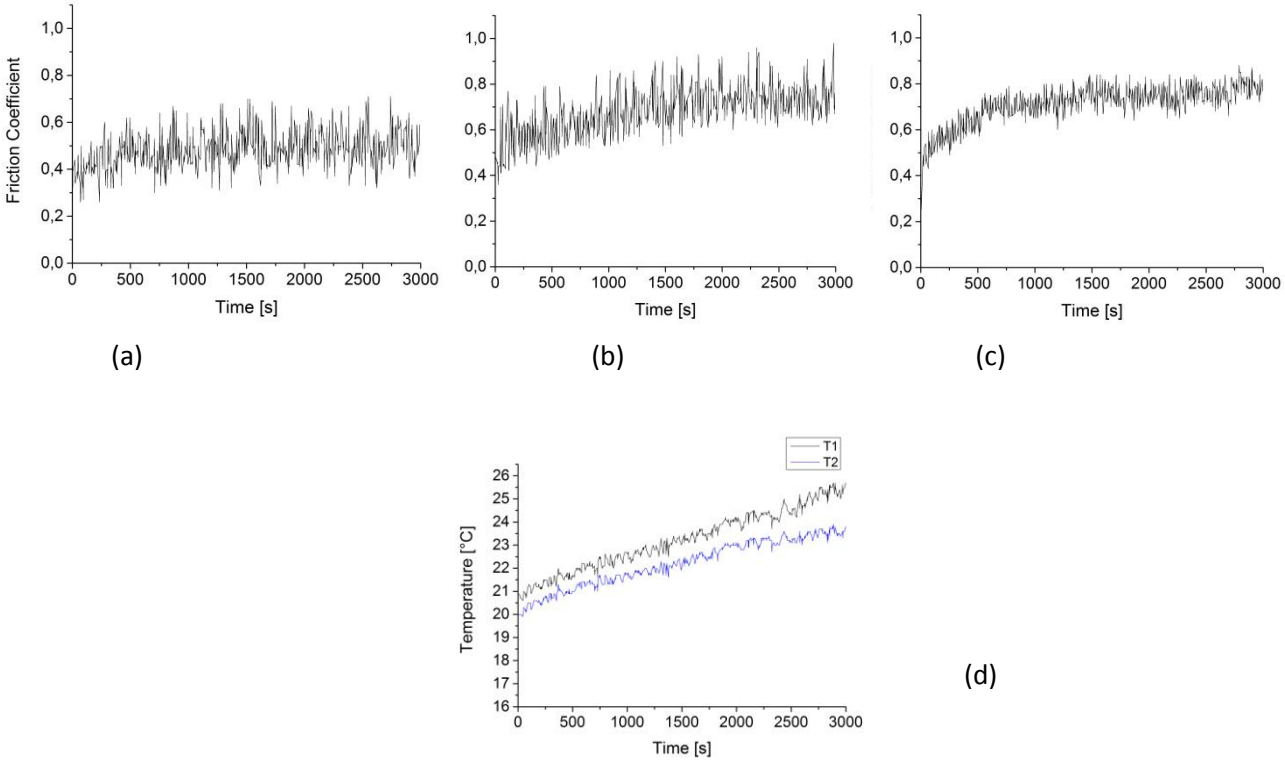

Fig. 3. friction coefficient during the pin on disc test of the discs with R_a 1 μm (a), 0.1 μm (b), 0.04 μm (c), (d) temperature profile recorded during the pin on disc test.

Table 2. pin on disc wear test results.

Coating Roughness Ra (μm)	Steady state friction coefficient	Wear Volume [mm^3]	Wear Rate [mm^3/mm]	Specific Wear Coefficient K_a [m^2/N]
5 μm	0.3 ± 0.1	49	$6\ 10^{-4}$	$2.10\ 10^{-11}$
1 μm	0.48 ± 0.1	2.02	$4.31\ 10^{-7}$	$1.49\ 10^{-14}$
0.1 μm	0.7 ± 0.1	1.46	$3.11\ 10^{-7}$	$1.06\ 10^{-14}$
0.04 μm	0.71 ± 0.08	1.05	$2.23\ 10^{-7}$	$7.64\ 10^{-15}$

3.3 Wear surfaces and cross sections

The pin wear surfaces were found to be characterized by the presence of distinct areas of the so-called friction layer, whose number and extension increases by decreasing the coating roughness. In Fig. 4, the worn pin surfaces for tests conducted against discs with the lowest and highest roughness are compared. The friction layers are quite different in the two cases. After sliding against disc with the lowest roughness (Fig. 4a), the pin friction layer is made by well compacted secondary plateau that form close to the metallic fibers (steel as well as copper fibers) that act as primary plateaus, i.e. as obstacles against which the wear fragments accumulate during sliding [5, 34-37]. Such plateaus tend also to spread over the metallic fibers. On the contrary, when sliding against the disc with R_a=5 μm (Fig. 4b), the pin worn surface is characterized by the presence of metallic fibers with severe abrasion traces. The corresponding secondary plateaus are quite limited in extension and made by less compacted particles. Moreover, as indicated by the EDXS analyses shown in Fig. 4c and d, the secondary plateaus are mainly made by wear fragments originating from the friction material since the EDXS spectra show the presence of the principal elements of the pin material. i.e. Zr, O, Si, Ti, Fe, Cu, Ca, Ba, K, Al. Pin surface obtained upon sliding against the disc with R_a= 0.04 μm, some material transfer from the coating to the pin surface was observed, as suggested by the presence of W, Co and Cr characteristics X-ray lines (arrowed in Figure 4c) in the EDXS spectrum. Secondary plateaus observed on the pin surfaces wear tested against disc with intermediate R_a (1 μm and 0.1 μm) have intermediate features, with more evident abrasion marks in the case of 1 μm coating roughness and a higher amount of material transfer when the coating roughness is 0.1 μm.

Observation of secondary plateaus was made also by the metallographic analysis of the pin cross-sections where the friction layers are clearly visible. Examples of friction layers are reported in Fig. 5. It is observed that the thickness of the friction layer increases by decreasing the surface roughness of the counterface disc. The EDXS analyses on the friction layers confirm the presence of some elements transferred from the coating (W and Co) on the pin tested against disc having R_a of 0.04-0.1 and 1 μm. No traces of W was found on the friction layer formed against the as-sprayed disc. The amount of W measured was seen to increase decreasing the coating roughness as reported in Table 3.

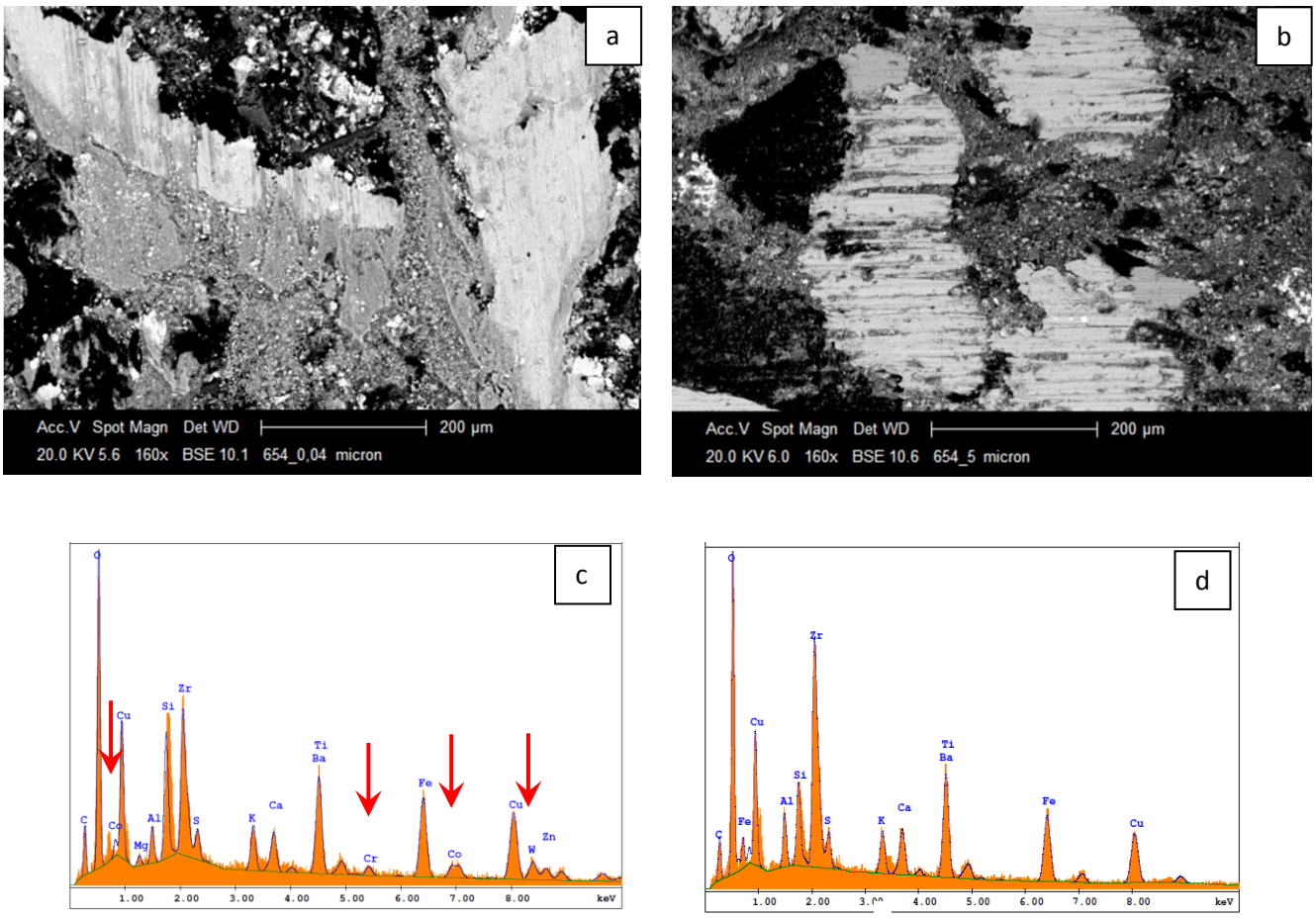

Fig. 4. Details of the pin surfaces, worn against disc with R_a=0.04µm (figure a) and Ra=5µm (figure b) and relevant EDXS analyses (c and d). The arrows indicate the characteristic X-ray lines of elements found in the friction layer on the pin surface after wear tests coming from the WC-CoCr disc coating.

Table 3. Tungsten concentration measured by EDXS on the fri . . . layer

Coating average roughness, µm	W (wt. %) measured by EDXS on the friction layer
5	0
1	3.7
0.1	7.3
0.04	11.3

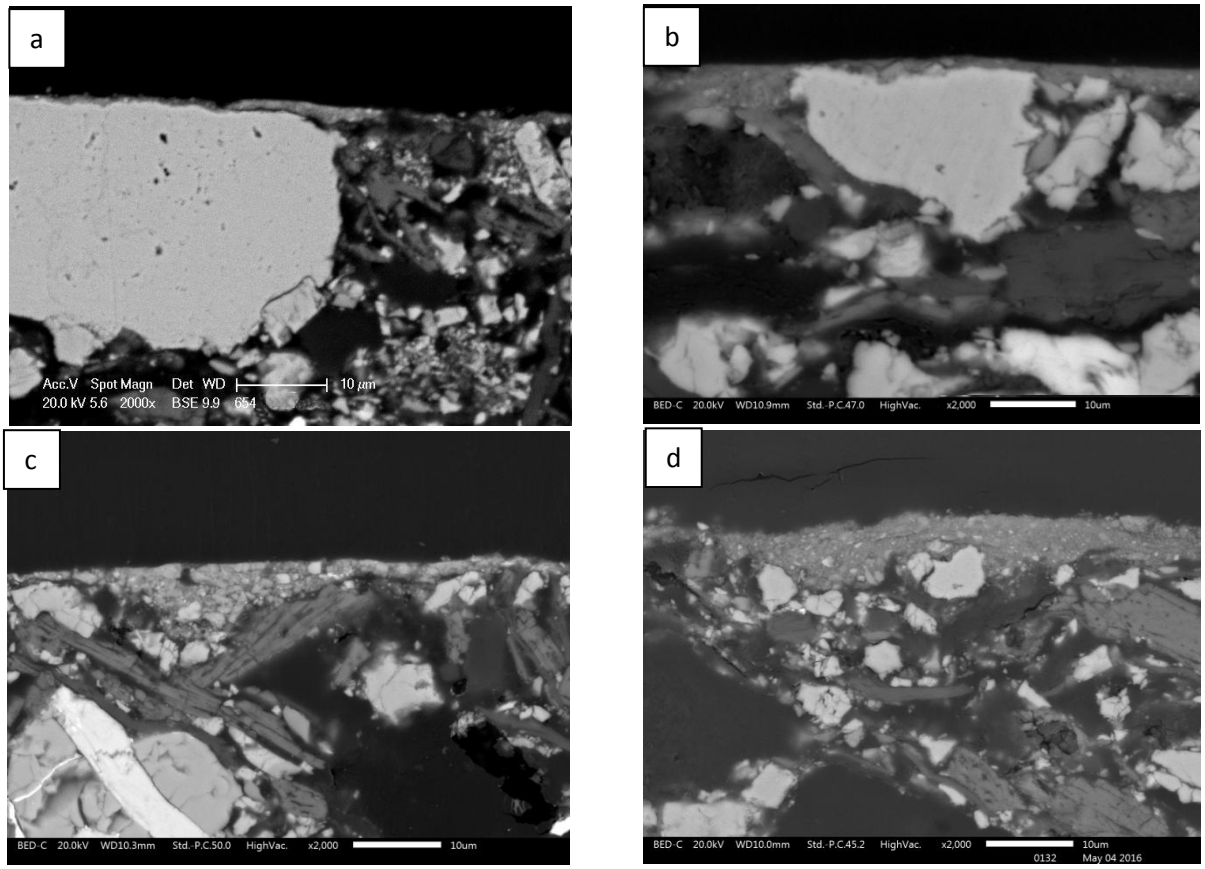

Fig. 5. cross-section of the pin worn against the discs with different R_a: (a) 5 μm, (b) 1 μm, (c) 0.1 μm, (d) 0.04 μm.

The disc wear surface observed in the SEM after the wear test are shown in Fig. 6. The comparison with the unworn surfaces (see Fig. 2b), allows us to understand the modifications introduced by sliding. It is worth starting commenting on the surface with R_a= 1 μm initial finish. The comparison of Fig.s 2b and 6b shows that after sliding, in addition to the white areas (coating polished asperities) and grey areas (coating unpolished regions) wide black areas can be observed. In Fig. 7 an observation of one of these areas at higher magnification is shown. The EDXS analysis taken in correspondence of the black area demonstrates that they are produced by the compaction of fragments originating from the friction material (pin) and then transferred onto the disc counterface. In particular fragments tend to pile-up preferentially into the valleys between the smoothed asperities, as schematized in Fig. 8. If the disc roughness is high (R_a= 5 μm), the amount of such transfer increases (see Fig. 6a). On the contrary, for lower disc surface roughness the amount of the transfer decreases, and it involves only small, limited areas, as shown by the black spots in Fig. 6c and d. The wear of the discs, evaluated by measuring the depth and extension of the wear track by a profilometer was negligible in all cases.

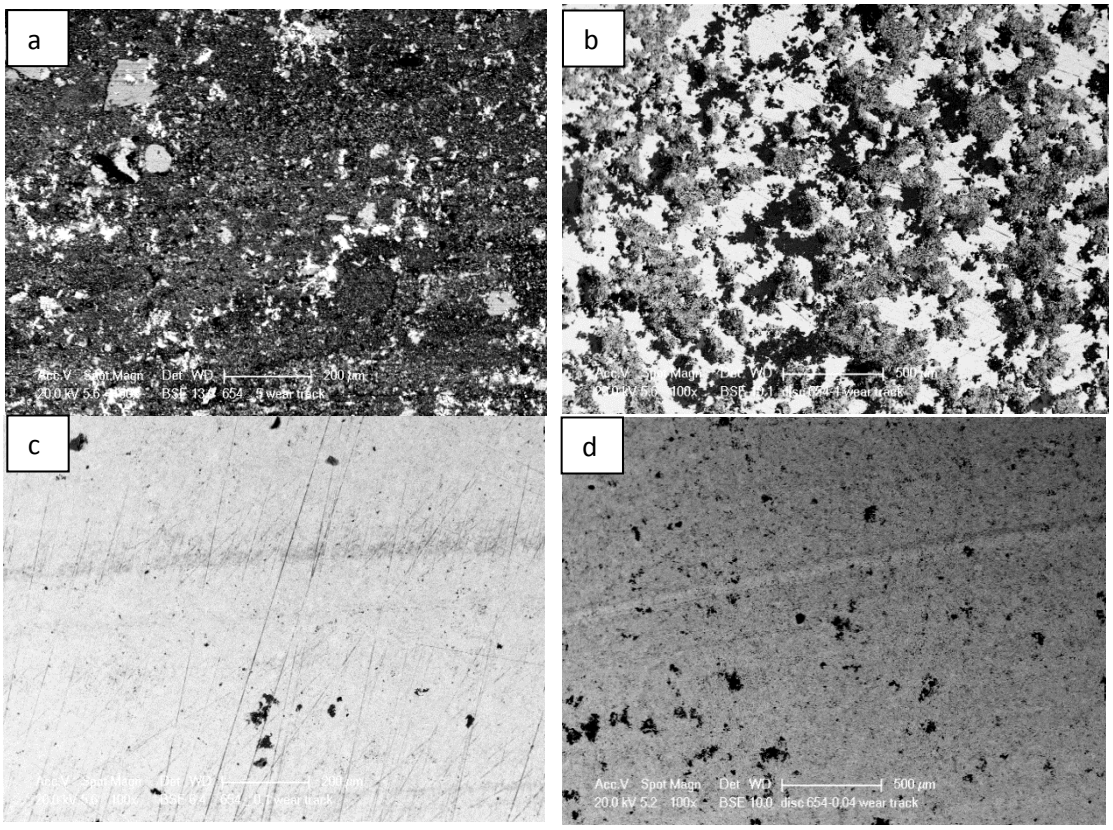

Fig. 6. Wear tracks on the discs with the following initial surface roughness, R_a: (a) 5 μm, (b) 1 μm, (c) 0.1 μm, (d) 0.04 μm.

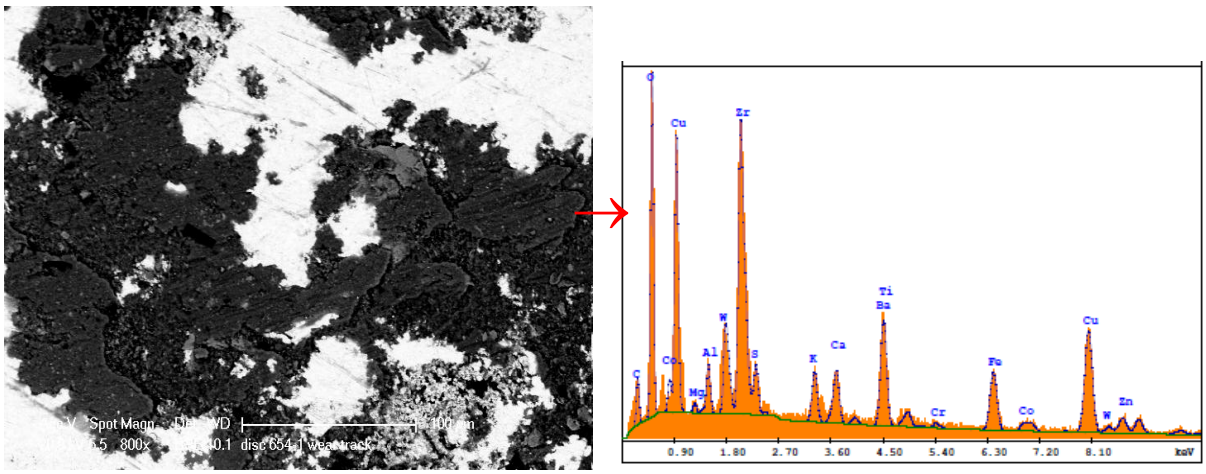

Fig. 7. Higher magnification SEM micrograph of Fig. 6b, showing the debris in between the polished asperities of the coating and relevant EDXS spectrum.

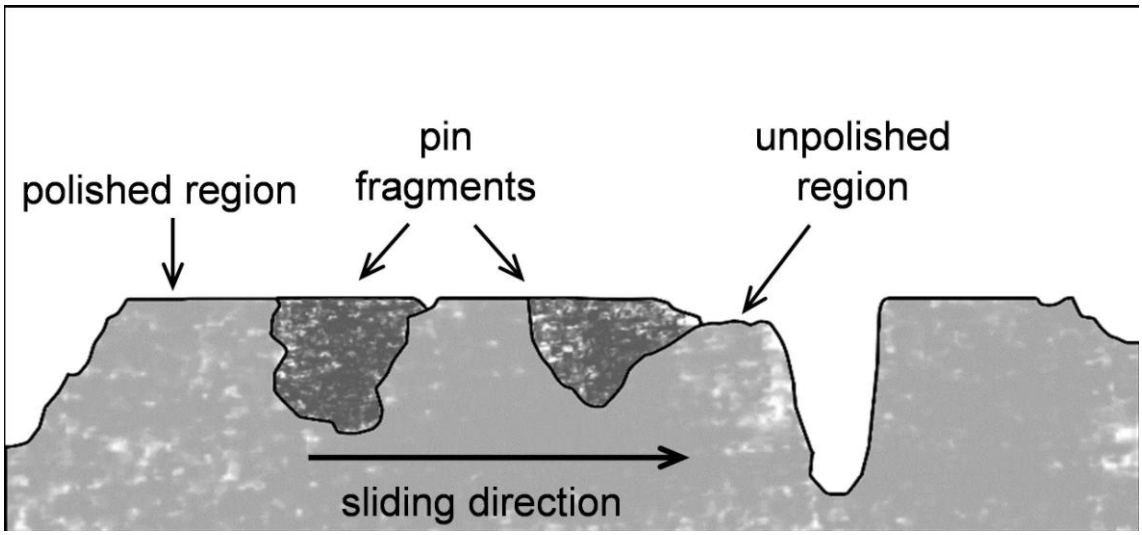

Fig. 8. Disc wear track profile: scheme of trapping of fragments from the pins.

4. Discussion

For a better understanding of the wear behavior of the tribological system under study, the wear rate and the friction coefficient in Table 2 are plotted against the coating roughness in Fig. 9. As can be observed, wear rate increases with roughness, with a big rise in passing from R_a=1 to 5 μm, while the steady-state coefficient of friction decreases with roughness. In order to explain these findings, it is important to consider the main features of the friction layer, summarized in Table 4 together with the corresponding wear mechanisms.

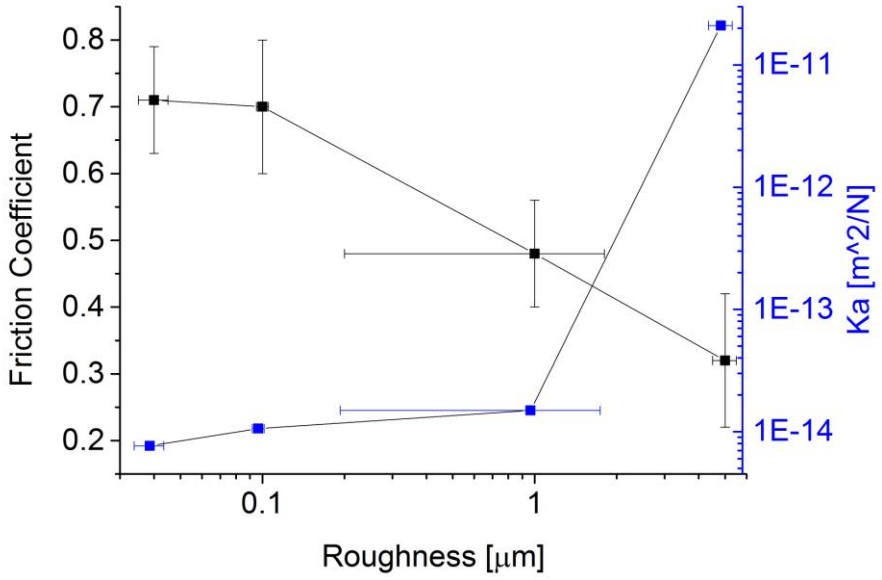

Fig. 9. Friction coefficient and wear rate vs. surface roughness

Table 4. Main characteristics of the friction layer

	Low disc roughness	High disc roughness
Pin	- Higher extension and thickness of the friction layer - Well compacted secondary plateau - High transfer of W from the counterface disc (it increases with decreasing roughness)	- Lower extension and thickness of the friction layer - Poor compacted secondary plateau - Low transfer of W (it is 0 at R_a=5 μm)
Disc	Low transfer from the pin counterface (only in the porosity)	Large transfer for R_a=1 μm and. in particular for R_a=5μm.

The friction layer that forms under sliding at the interface between a friction material and a counterface disc is made by primary and secondary plateaus [34-37]. In general the primary plateaus are made by large and hard constituent of the friction material, such as metallic fibers and ceramic particles, whereas the secondary plateaus are formed by the compaction of wear fragments blocked by the primary plateaus. Wear fragments would originate from the friction material as well as the counterface disc. In case of conventional discs, made by pearlitic cast iron, the disc largely contributes to the formation of the secondary plateau and also to wear fragments. In fact, the iron fragments get oxidized during sliding and enter the secondary plateau in the form of iron oxides. In the present study, the primary plateaus are mainly made by the metallic fibers, i.e. the steel and copper fibers. Since the counterface disc is coated with a cermet that do not provide a large amount of wear fragments, the extension of the friction layer, and in particular of the secondary plateau, is much more limited than in the case of the uncoated discs and it is almost exclusively made of wear debris from the friction material. A certain amount of fragments from the coating, as proved by the presence in the friction of W, Co and Cr (see Fig. 4c) is also observed, increasing as disc roughness is decreased (Table 3). As concerns W, this elements might be present in two forms: metallic or as a carbide. Elemental tungsten may diffuse from the coating due to the close contact between the pin and the disc sliding surfaces if the temperature was sufficiently high [45]. In the present system, small WC particles are released when the Co-Cr binder is worn out [28, 46].

From the above friction and wear results some conclusions can be drawn on the main acting wear mechanisms. The wear behavior of the tribological system seems to be dominated by abrasive and adhesive interactions at the contact regions. In case of the tests with the disc in the as-sprayed condition (R_a=5 μm), the abrasive interactions between the hard asperities of the disc coating and the quite soft friction material are prevailing. Such abrasive interactions are also evidenced by the presence of scratches on the surface of the fibers acting as primary plateaus. The corresponding wear rate is really severe, owing to the large removal of material from the surface of the friction layer and its transfer onto the disc surface in the regions between the asperities. On the contrary, the friction coefficient is relatively low. This can be explained by considering that in general the friction coefficient can be expressed by the two contributions [12]:

$$\mu = \mu_{abr} + \mu_{ad}$$

where the subscripts “abr” and “ad” indicate the abrasive and adhesive contributions, respectively. The abrasive contribution is related to the interactions described above, among the coating asperities and the friction material. Using the model proposed, using the model by Rabinowicz [47]: $\mu_{abr}=tg\Theta$, where Θ is the average attack angle that the asperities form with the sliding surface. We do not have an estimation of Θ, but even in very rough surfaces Θ does not exceed 10° [12]. Therefore μ_{abr} should not exceed 0.2 at most. The remaining part of μ is given by the adhesive interaction between the ceramic asperities of the coating and the friction material. This contribution is given by $\mu_{ad}= \tau_m A_r/F_N$, where τ_m is the average shear stress to separate the contacting asperities (approximately proportional to the work of adhesion [12, 48]). A_r is the real area of contact and F_N is the applied load. The contribution of μ_{ad} is thus expected to be limited when the coating has its original roughness, since A_r is quite low. The real area of contact between the two mating surfaces is mainly determined by the dimension of the primary plateaus that would sustain most of the load since the compactness of the secondary plateaus is quite poor.

As the coating roughness is reduced, the wear rate decreases and the friction coefficient rises. This behavior is determined by the progressive reduction of the abrasion contribution to wear, as the disc roughness passes from the initial R_a=5 μm to a roughness of 1 μm or lower. Indeed, the smoothening of the highest coating asperities results in a strong decrease of the pin wear rate. For R_a-values lower or equal than 1 μm, wear rate becomes substantially similar to the typical values displayed by this material when sliding against a cast iron counterface [5, 9, 22]. At the same time, by reducing the coating roughness, the adhesive interaction between pin and disc strongly increases and this induces an increase in the friction coefficient. In fact, by decreasing the disc roughness the extension of the friction layer increases and the compactness of the secondary plateaus increases as well (see the summary in Table 3). Both effects contribute to increase the real area of contact, thereby μ_{ad}. With decreasing roughness, μ_{abr} decreases in importance but this trend is clearly overwhelmed by the increase in μ_{ad}. Such an increase in A_r and in friction is also coherent with the observed increase of tungsten concentration (see Table 3) with decreasing coating roughness in the friction layer building up on the pin surface. To summarize, the lower the coating roughness, the more extended the friction layer because it is not abraded (i.e. destroyed) by the coating asperities. On the contrary, in case of very high roughness, as in the as-sprayed conditions, the extremely severe abrasion acted by the much higher and sharper coating asperities on the softer pin material prevents the accumulation and compaction of the wear debris and the formation of both primary and secondary plateaus. The coating in this case does not release any WC particle being not consumed by adhesive wear against the pin surface. The high values of the friction coefficient recorded in this study for smoother coating surface finish are similar to those reported by Usmani et al. [25] during PoD tests (in the ball-on-flat configuration) with different WC-Co coatings against a 440C steel. An important adhesive contribution to wear was also in the cited study the ruling mechanism.

5. Conclusions

The wear behavior of a WC-CoCr HVOF coated disc having different surface roughness tested in dry sliding against a commercial brake pad material was evaluated and interpreted considering the peculiar features of the friction layer that forms during sliding on the pin and the characteristics of the disc wear tracks. The main findings are summarized as follows:

- the main constituents of the friction layer are not Fe oxides, as observed when the same pad material was tested against an uncoated cast iron disc, but ZrO_2, Cu and all the other components of the friction material;
- in case of the tests using the coated disc in the as-sprayed condition, the wear is extremely severe and the friction coefficient is quite low, because of the prevailing abrasive interactions in the contact regions;
- decreasing the surface roughness, the abrasive interactions become less important; as a consequence, an increase in the extension and thickness of the friction layer is observed that in turn increases the adhesive interactions in the contact regions;
- decreasing the surface roughness also increases tungsten concentration in the friction layer transferred from the coating, for an increase of the adhesive component of the tribological coupling;
- if the coating roughness is lower or equal than 1 μm, the pin wear rate is mild and very similar to that displayed when sliding against a cast iron disc, whereas the disc wear rate is negligible.

The results of the PoD tests using coatings with surface roughness in the range of 0.1 – 1 μm are very promising, in terms of friction coefficient, which is adequately high, and wear rate that is adequately low (negligible in the case of the disc) in view of brake applications. The low system wear is also promising with regard to the reduction of PM emission in the atmosphere. Of course, specific dyno or bench-tests would be highly recommended in order to confirm the obtained results and for evaluating the performance of real braking systems.

Acknowledgments

The research leading to these results has achieved funding from the European Union Seventh Framework Programme (FP-PEOPLE-2012-IAPP) under the Rebrake Project, grant agreement no. 324385 (www.rebrake-project.eu).

References

1. P. Sanders, N. Xu, T.M. Dalka, M.M. Maricq, Airborne brake wear debris: size distributions, composition,and a comparison of dynamometer and vehicle tests, Environ.Sci.Technol.37 (2003) 4060−4069.
2. J. Wahlstrom, L. Olander, U. Olofsson, A pin-on-disc study focusing on how different load levels affect the concentration and size distribution of airborne wear particles from the disc brake materials, Tribol. Lett. 46 (2012) 195−204.
3. G. Straffelini, R. Ciudin, A. Ciotti, S. Gialanella, Present knowledge and perspectives on the role of copper in brake materials and related environmental issues: A critical assessment, Environmental Pollution, 207 (2015) 211-219.
4. J. Kukutschova, V. Roubicek, K. Malachova, Z. Pavlickova, R. Holusa, J. Kubackova, V. Micka, D. MacCrimmon, P. Filip, Wear mechanism in auto- motive brake materials, wear debris and its potential environmental impact, Wear 267 (2009) 807−817.
5. P.C. Verma, L. Menapace, A. Bonfanti, R. Ciudin, S. Gialanella, G. Straffelini, Braking pad-disc system: wear mechanisms and formation of wear fragments, Wear 322−323 (2015) 251−258.

6. N. Aranganathan, J. Bijjwe, Development of copper-free eco-friendly brake-friction material using novel ingredients, 352-253 (2016) 79-91.
7. K.W. Hee, P. Filip, Performance of ceramic enhanced phenolic matrix brake lining materials for automotive brake linings, Wear 259 (2005) 1088-1096.
8. J. Bijwe, Composites as friction materials: recent developments in non- asbestos fiber reinforced friction materials – a review, Polym.Compos.18 (1997) 378–396.
9. A.E. Anderson, Friction and wear of automotive brakes, ASM Handbook,vol.18, 1992, 569–577.
10. G. Straffelini. P.C. Verma, I. Metinoz, R. Ciudin, G. Perricone, S. Gialanella, Wear behavior of a low metallic friction material dry sliding against a cast iron disc: Role of the heat-treatment of the disc. Wear 348-349 (2016) 10–16.
11. R.J.K. Wood, Tribology of thermal sprayed WC-Co coatings, Int. J. Refract. Met. H.. 28 (2010). pp. 82–94.
12. G. Straffelini, Friction and Wear, Methodologies for Design and Control, Springer International Publishing Switzerland, 2015.
13. H.L. De Villiers Lovelock, Powder/processing/structure relationships in WC–Co thermal spray coatings: a review of the published literature, J. Therm. Spray. Technol. 7 (1998) 357–373.
14. M.R. Dorfman, B.A. Kushner, J. Nerz, A.J. Rotolico, A technical assessment of high velocity oxygen-fuel versus high energy plasma tungsten carbide–cobalt coatings for wear resistance, in: Proceedings of the 12th International Thermal Spray Conference, London, 1989, pp. 291–302.
15. R. Schwetzke, H. Kreye, Microstructure and properties of tungsten carbide coatings sprayed with various HVOF spray systems, in: C. Coddet (Ed.), Thermal Spray: Meeting the challenges of the 21st century, ASM Int., Materials Park, OH, USA, 1998, 187–192.
16. J.A. Peters , F. Ghasripoor, Sliding Wear Behavior of Carbide Coatings ," in *Thermal Spray Industrial Applications* , C.C. Berndt and S. Sampath, eds., ASM International, Materials Park, OH, pp 387 – 392 (1995).
17. S.F. Wayne, S. Sampath, Structure/Property Relationships in Sintered and Thermally Sprayed WC-Co , Jour. Ther. Spray Tech., 1 , 4 , (1992) 307 – 315.
18. V. Ramnath, N. Jayaraman, Characterization and Wear Performance of Plasma-Sprayed WC-Co Coatings, *Mat. Sci. Tech.*, 5 , 4, (1989), 382 – 388.
19. Y. Naerheim, C. Coddet, P. Droit, Effect of Thermal Spray Process Selection on Tribological Performance of WC-Co and Al_2O_3-TiO_2 Coatings, *Surface Eng*., 11 , 1 , (1995), 66 – 70.
20. J. Nerz, B. Kushner, A. Rotolico, Microstructural Evaluation of Tungsten Carbide-Cobalt Coatings, Jour. Ther. Spray Tech., 1, 2, (1992), 147 – 152.
21. J. Kraak, W. Herlaar, J. Wolke, K. de Groot, E. Jr. Hyduk, Influence of Different Gases on the Mechanical and Physical Properties on HVOF Sprayed Tungsten Carbide Coatings, in *Thermal Spray: International Advances in Coatings Technology*, Berndt C. C. ed., ASM International , Materials Park , OH , pp 153 – 158 (1992).
22. G. Straffelini, L. Maines, The relationship between wear of semimetallic friction materials and pearlitic cast iron in dry sliding, Wear 307 (2013) 75-80.
23. H. Wang; X. Wang. X. Song. X. Liu. X. Liu: Sliding wear behavior of nanostructured WC-Co-Cr coatings. Applied Surface Science. Volume 355. p. 453-460.
24. Q. Yang, T. Senda, A. Ohmori, Effect of carbide grain size on microstructure and sliding wear behavior of HVOF-sprayed WC-12% Co coatings, Wear 254 (2003) 23–34.
25. S. Usmani, S. Sampath, D.L. Houck, D. Lee, Effect of carbide grain size on the sliding and abrasive wear behavior of thermally sprayed WC-Co coatings, Tribology Transactions, 40 (1997) 470–478.

26. A.H. Dent, S. de Palo, S. Sampath, Examination of the wear properties of HVOF sprayed nanostructured and conventional WC-Co cermets with different binder phase contents, J. Therm. Spray Technol. 11 (2002) 551–558.
27. J. He, J.M. Schoenung, Nanostructured coatings, Mater. Sci. Eng. A Struct. 336 (2002) 274–319
28. P.H. Shipway, D.G. McCartney, T. Sudaprasert, Sliding wear behaviour of conventional and nanostructured HVOF sprayed WC-Co coatings, Wear 259 (2005) 820–827.
29. Y. Ishikawa, S. Kuroda, J. Kawakita, Y. Sakamoto, M. Takaya, Sliding wear properties of HVOF spayed WC-20%Cr_3C_2-7%Ni cermet coatings, Surface & Coatings Technology 201 (2007) 4718-4727.
30. G. Bolelli, L.M. Berger, M. Bonetti, L. Lusvarghi, Comparative study of the dry sliding wear behavior of HVOF-sprayed WC-$(W,Cr)_2C$-Ni and WC-Co hardmetal coatings, Wear 309 (2014) 96-111.
31. Y. Ishikawa, J. Kawakita, S. Osawa, T. Itsukaichi, Y. Sakamoto, M. Takaya, S. Kuroda, Evaluation of Corrosion and Wear Resistance of Hard Cermet Coatings Sprayed by Using an Improved HVOF Process, Journal of Thermal Spray Technology, 14 (3), 2005, 384-390.
32. G.C. Saha, T.I. Khan, The corrosion and wear performance of microcrystalline WC-10Co-4Cr and near-nanocrystalline WC-17Co high velocity oxy-fuel sprayed coatings on steel substrate, Metallurgical and Materials transactions A, vol.41A, 3000-3009.
33. M. Watremaz, J.P. Bricout, B. Marguet, J. Oudin, Friction, Temperature, and Wear Analysis for Ceramic Coated Brake Disks, ASME Journal of Tribology, 118 (1996) 457-465.
34. W. Osterle, I. Urban,T hird body formation on brake pads and rotors, Tribol. Int. 39 (2006) 401–408.
35. W. Osterle, I. Urban, Friction layers and friction films on PMC brake pads, Wear 257 (2004) 215–226.
36. P. Filip, Z. Weiss, D. Rafaja, On friction layer formation in polymer matrix composite materials for brake applications, Wear 252 (2002) 189–198.
37. M. Eriksson, S. Jacobson, Tribological surfaces of organic brake pads, Tribol. Int. 33 (2000) 817–827.
38. G.M. La Vecchia, F. Mor, G. Straffelini, D. Doni, Microstructure and sliding wear behavior of thermal spray carbide coatings, The International Journal of Powder Metallurgy, 35 (1999) 37-46.
39. F. Mor, G.M. La Vecchia, D. Stehle, Caratterizzazione di Riporti Thermal Spray Ottenuti con Sistema HVOF al Variare dei Parametri di Processo, La Met. It., 88 (1996) 363-370.
40. P.C. Verma, R. Ciudin, A. Bonfanti, P. Aswath, G. Straffelini, S. Gialanella, Role of the friction layer in the high-temperature pin-on-disc study of a brake material, Wear 346-347 (2016) 56–65.
41. C. Verdon. A. Karimi. J.-L. Martin, A study of high velocity oxy-fuel thermally sprayed tungsten carbide based coatings. Part 1: microstructures, Mater. Sci. Eng. A. 246 (1998) 11–24.
42. J. Yuan. Q. Zhan. J. Huang. S. Ding. H. Li, Decarburization mechanisms of WC-Co during thermal spraying: insights from controlled carbon loss and microstructure characterization, Mater. Chem. Phys.142 (2013) 165–171.
43. G. Straffelini, S. Verlinski, P.C. Verma, G. Valota, S. Gialanella, Wear and contact temperature evolution in Pin-on-Disc tribotesting of low-metallic friction material sliding against pearlitic cast iron, Tribology Letter 62 (2016) 36-47.
44. K. Bode, G.P. Ostermayer, A comprehensive approach for the simulation of heat and heat-induced phenomena in friction materials, Wear 311 (2014) 47-56.
45. Gopal S. Upadhyaya, Cemented Tungsten Carbides: production, properties and testing, Noyes Publications, Westwood New Jersey, USA.

46. J. Pirso, S.Letunovits, M.Viljus, Friction and wear behavior of cemented carbides, wear 257 (2004) 257-265.
47. E. Rabinowicz, Friction and wear of materials, 2nd edition, Wiley.
48. G. Straffelini, A simplified approach to the adhesive theory of friction, Wear 249 (2001) 79-85.

Tables

Table 1.

Surface finish of the coated discs.

Final roughness R_a (μm)	Surface finish
5	As sprayed
1	Diamond disc (220 grit) – 30 s
0.1	Diamond disc (220 grit) – 2 min.
0.04	Diamond disc (220 grit) – 2 min. Diamond disc (1200 grit) – 5 min. Cloth + 9 μm diamond paste – 15 min. Cloth + 6 μm diamond paste – 15 min. Cloth + 3 μm diamond paste – 15 min.

Table 2.

Pin on disc wear test results.

Coating Roughness Ra (μm)	**Steady state friction coefficient**	**Wear Volume [mm^3]**	**Wear Rate [mm^3/mm]**	**Specific Wear Coefficient K_a [m^2/N]**
5 μm	0.3 ± 0.1	49	$6\ 10^{-4}$	$2.10\ 10^{-11}$
1 μm	0.48 ± 0.1	2.02	$4.31\ 10^{-7}$	$1.49\ 10^{-14}$
0.1 μm	0.7 ± 0.1	1.46	$3.11\ 10^{-7}$	$1.06\ 10^{-14}$
0.04 μm	0.71 ± 0.08	1.05	$2.23\ 10^{-7}$	$7.64\ 10^{-15}$

Table 3. Tungsten concentration measured by EDXS on the friction layer

Coating average roughness, μm	W (wt. %) measured by EDXS on the friction layer
5	0
1	3.7
0.1	7.3
0.04	11.3

Table 4. Main characteristics of the friction layer

	Low disc roughness	High disc roughness
Pin	- Higher extension and thickness of the friction layer - Well compacted secondary plateau - High transfer of W from the counterface disc (it increases with decreasing roughness)	- Lower extension and thickness of the friction layer - Poor compacted secondary plateau - Low transfer of W (it is 0 at R_a=5 μm)
Disc	Low transfer from the pin counterface (only in the porosity)	Large transfer for R_a=1 μm and. in particular for R_a=5μm.

Figure captions

Fig. 1. Example of cross section of a cast iron disc coated with a WC-CoCr layer. (a) Low magnification; (b) high magnification.

Fig. 2. Initial disc surfaces. (a) R_a=5 μm, (b) R_a=1 μm, (c) R_a=0.1 μm, (d) R_a=0.04 μm, (e) schematic of the effect of grinding/polishing.

Fig. 3. friction coefficient during the pin on disc test of the discs with R_a 1 μm (a), 0.1 μm (b), 0.04 μm (c), (d) temperature profile recorded during the pin on disc test.

Fig. 4. Details of the pin surfaces, worn against disc with R_a=0.04μm (figure a) and Ra=5μm (figure b) and relevant EDXS analyses (c and d). The arrows indicate the characteristic X-ray lines of elements found in the friction layer on the pin surface after wear tests coming from the WC-CoCr disc coating.

Fig. 5. cross-section of the pin worn against the discs with different R_a: (a) 5 μm, (b) 1 μm, (c) 0.1 μm, (d) 0.04 μm.

Fig. 6. Wear tracks on the discs with the following initial surface roughness, R_a: (a) 5 μm, (b) 1 μm, (c) 0.1 μm, (d) 0.04 μm.

Fig. 7. Higher magnification SEM micrograph of Fig. 6b, showing the debris in between the polished asperities of the coating and relevant EDXS spectrum.

Fig. 8. Disc wear track profile: scheme of trapping of fragments from the pins.

Fig. 9. Friction coefficient and wear rate vs. surface roughness

***Suggested Reviewers**

Click here to download Suggested Reviewers: Suggested reviewers.doc

Suggested reviewers

1) Peter Filip

Center for Advanced Friction Studies, Carbondale (US)

filip@siu.edu

Recognized expert in the friction and wear of braking systems.

2) Maria D. Salvador

Instituto de Tecnologia de Materialesm Universidad Politecnica de Valencia, Spain

dsalva@mcm.upv.es

Expert in thermal coatings and their characterization (including wear behavior).

3) Werner Oesterle

BAM Bundesanstalt Mat Forsch & Prufung

Werner.oesterle@ban.de

Recognized expert in braking systems as well as in tribology in general.

Figure 1a

Click here to download high resolution image

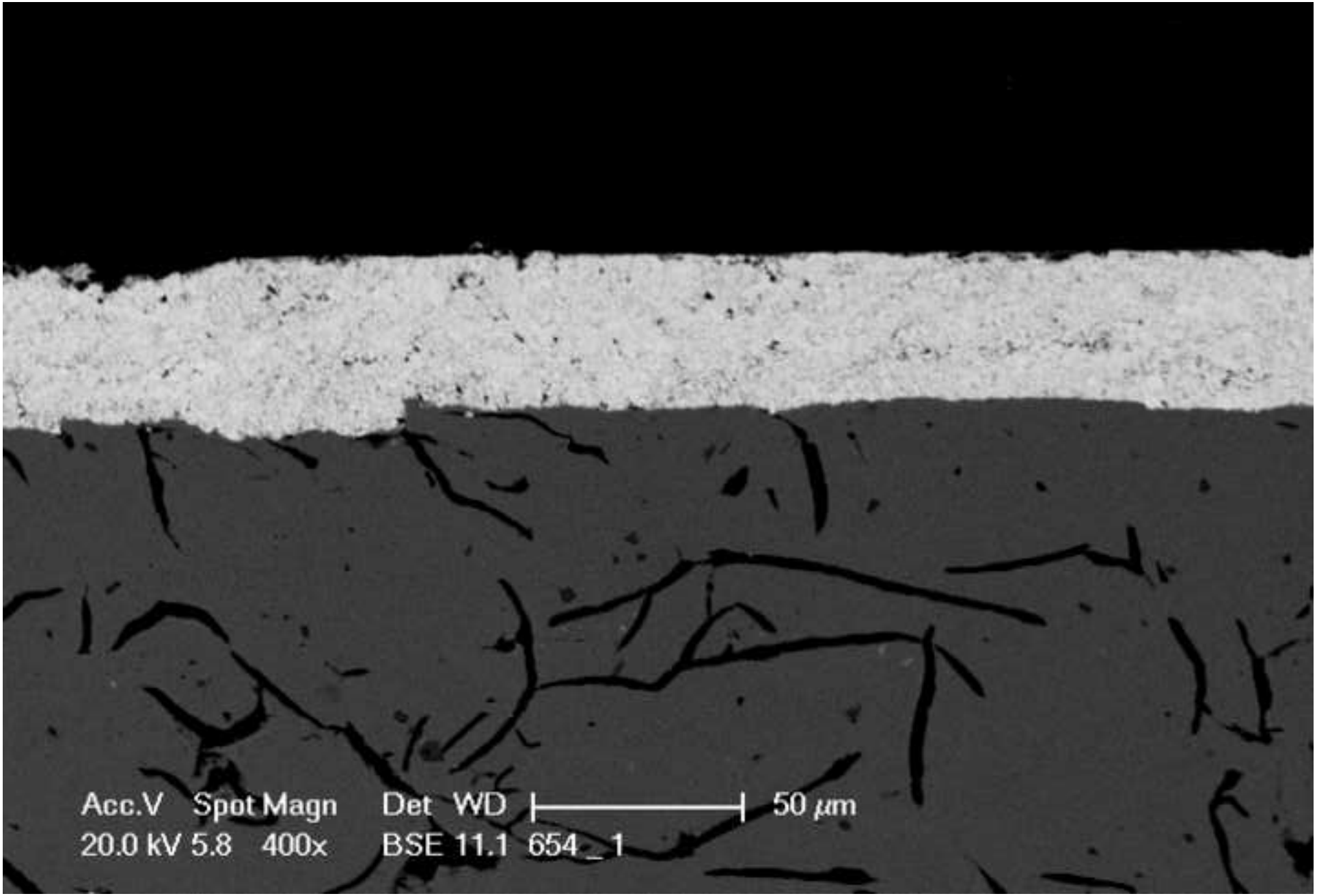

Figure 1b

Click here to download high resolution image

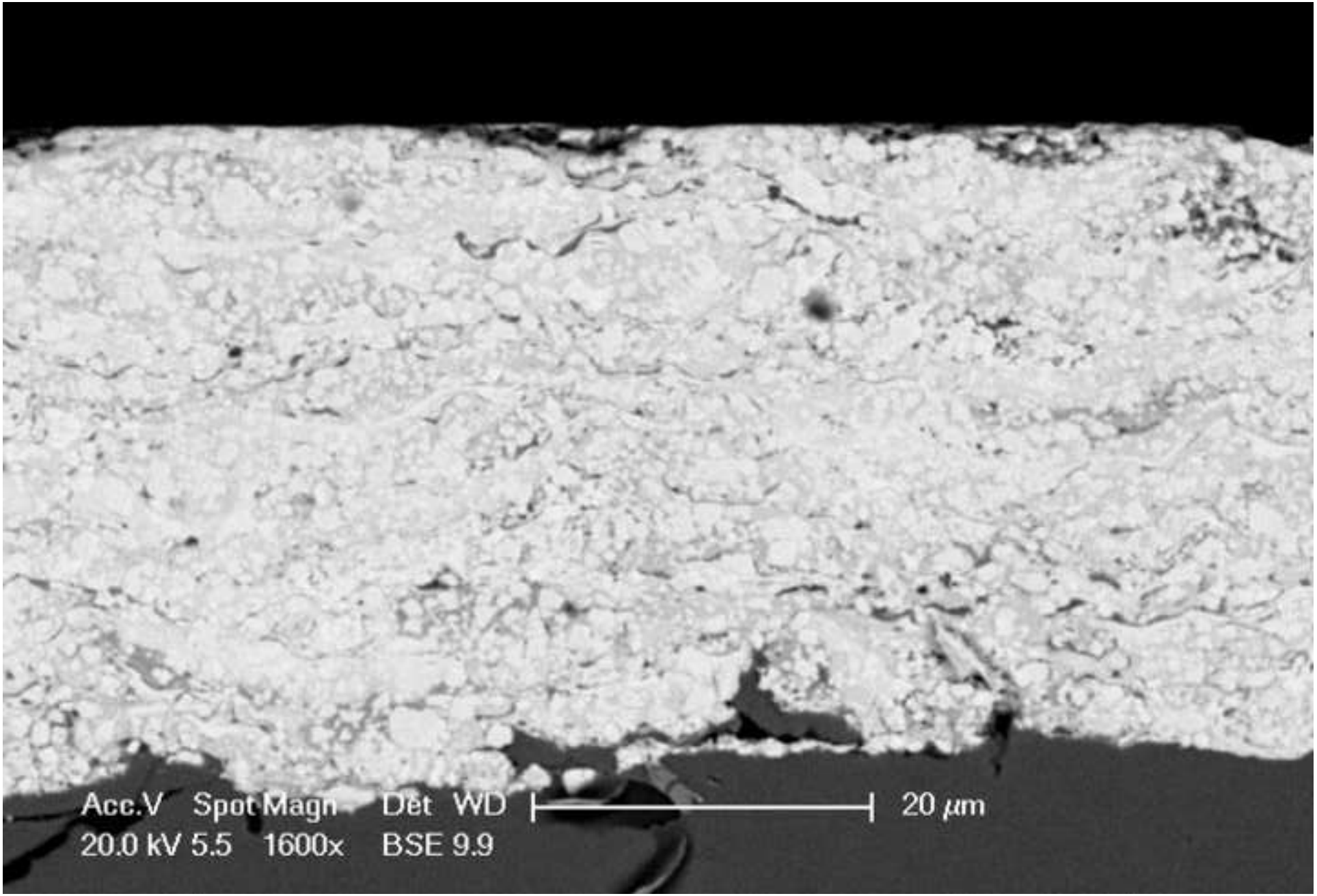

Figure 2a

Click here to download high resolution image

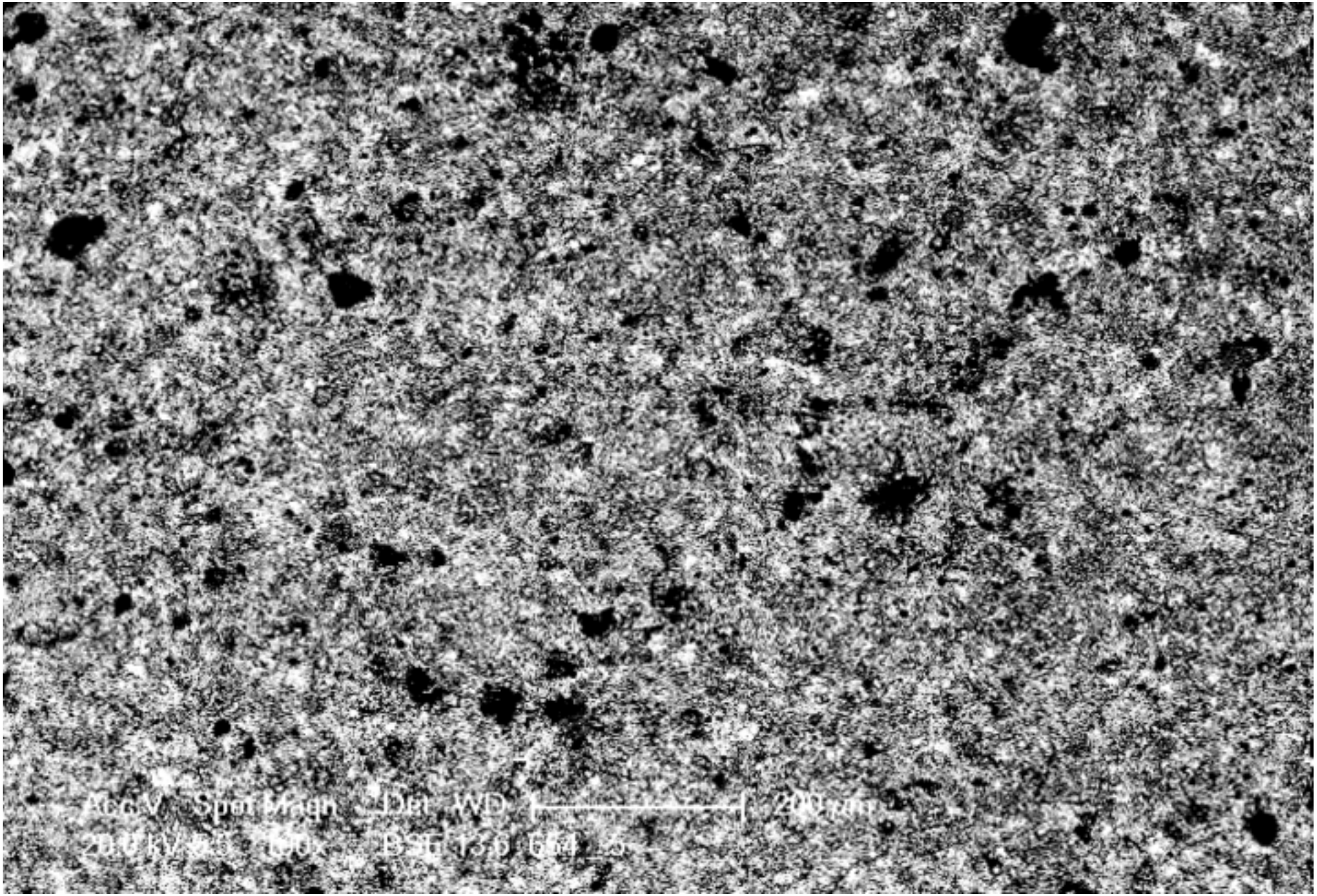

Figure 2b

Click here to download high resolution image

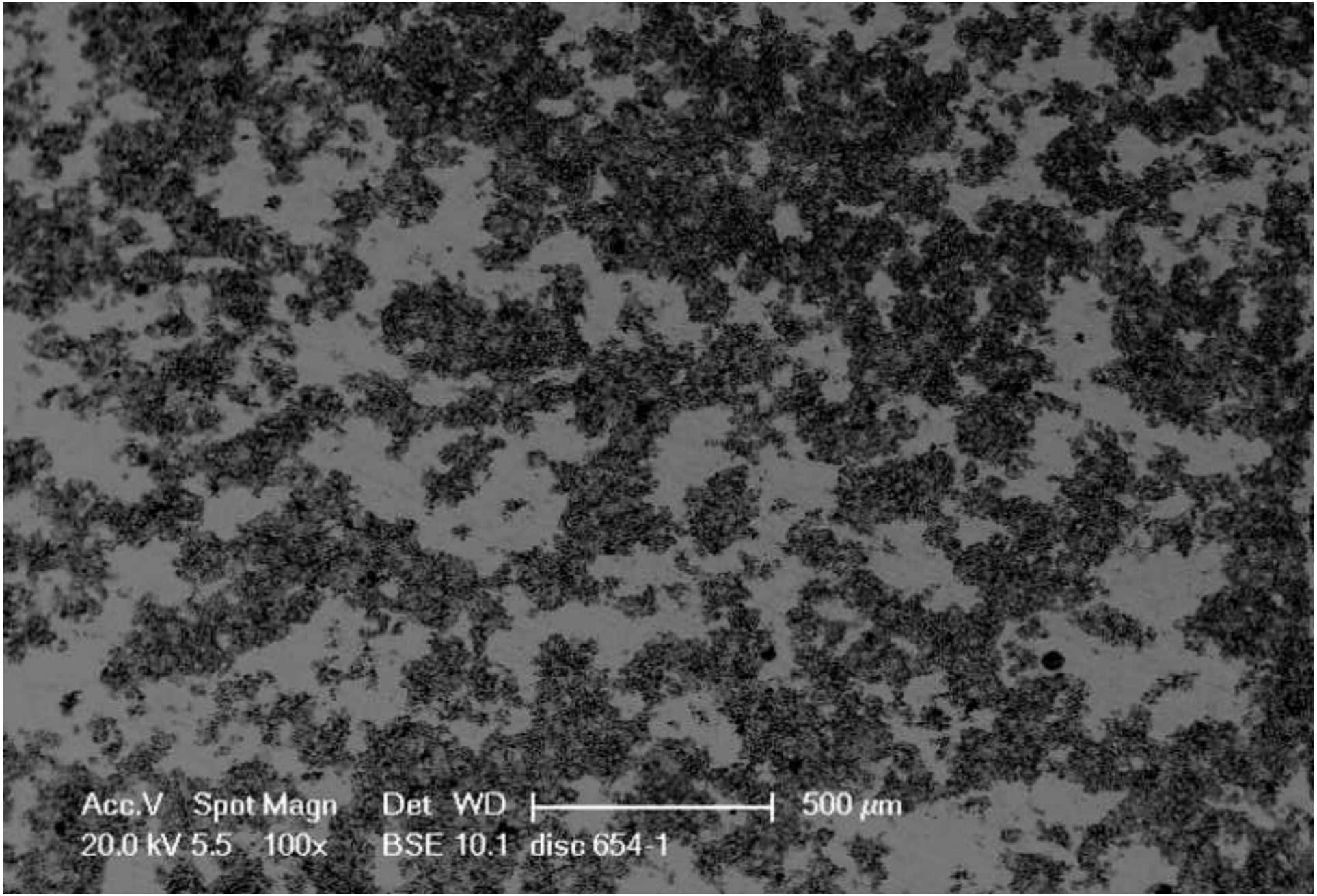

Figure 2c

Click here to download high resolution image

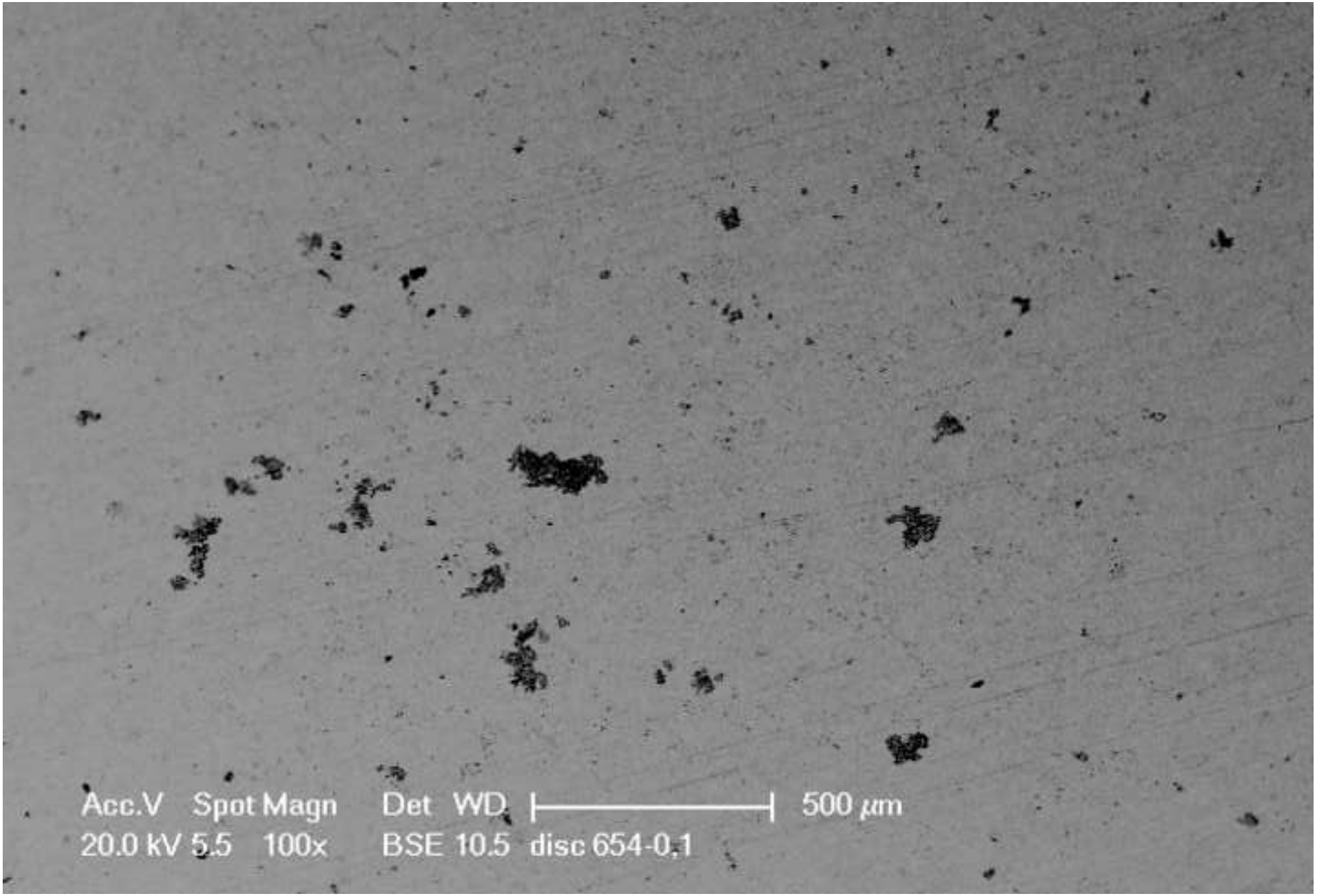

Figure 2d

Click here to download high resolution image

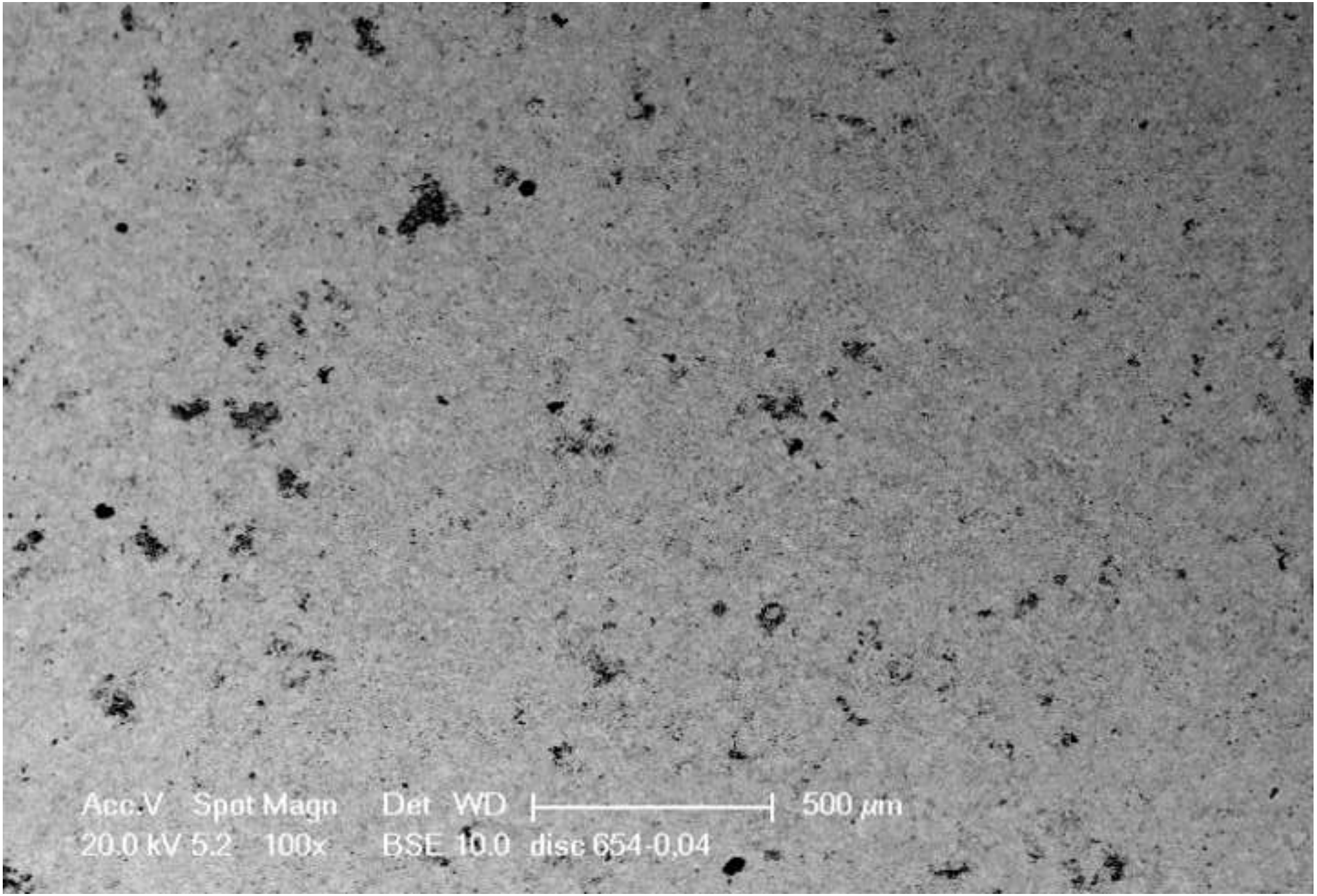

Figure 2e
Click here to download high resolution image

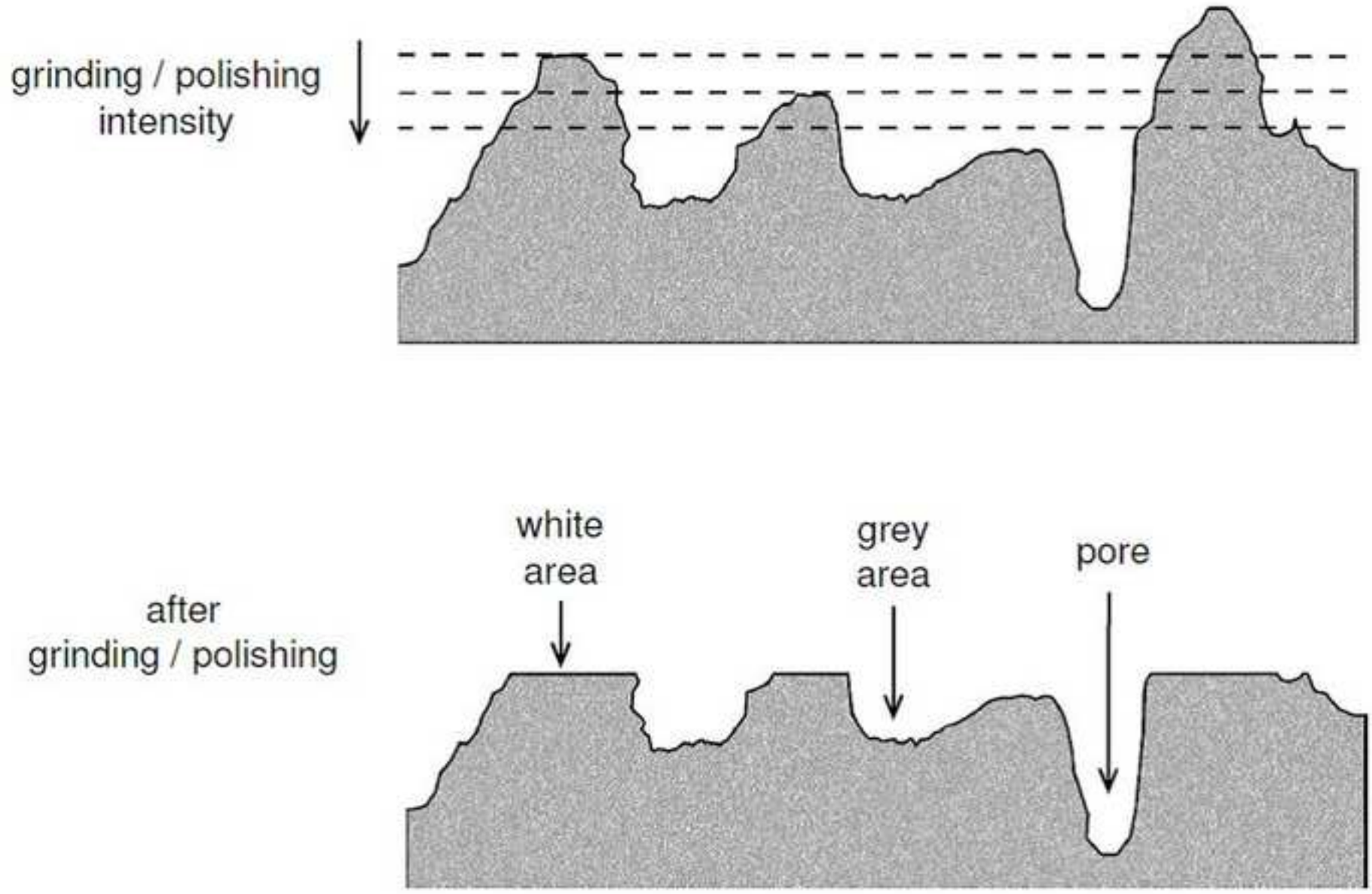

Figure 3a
Click here to download high resolution image

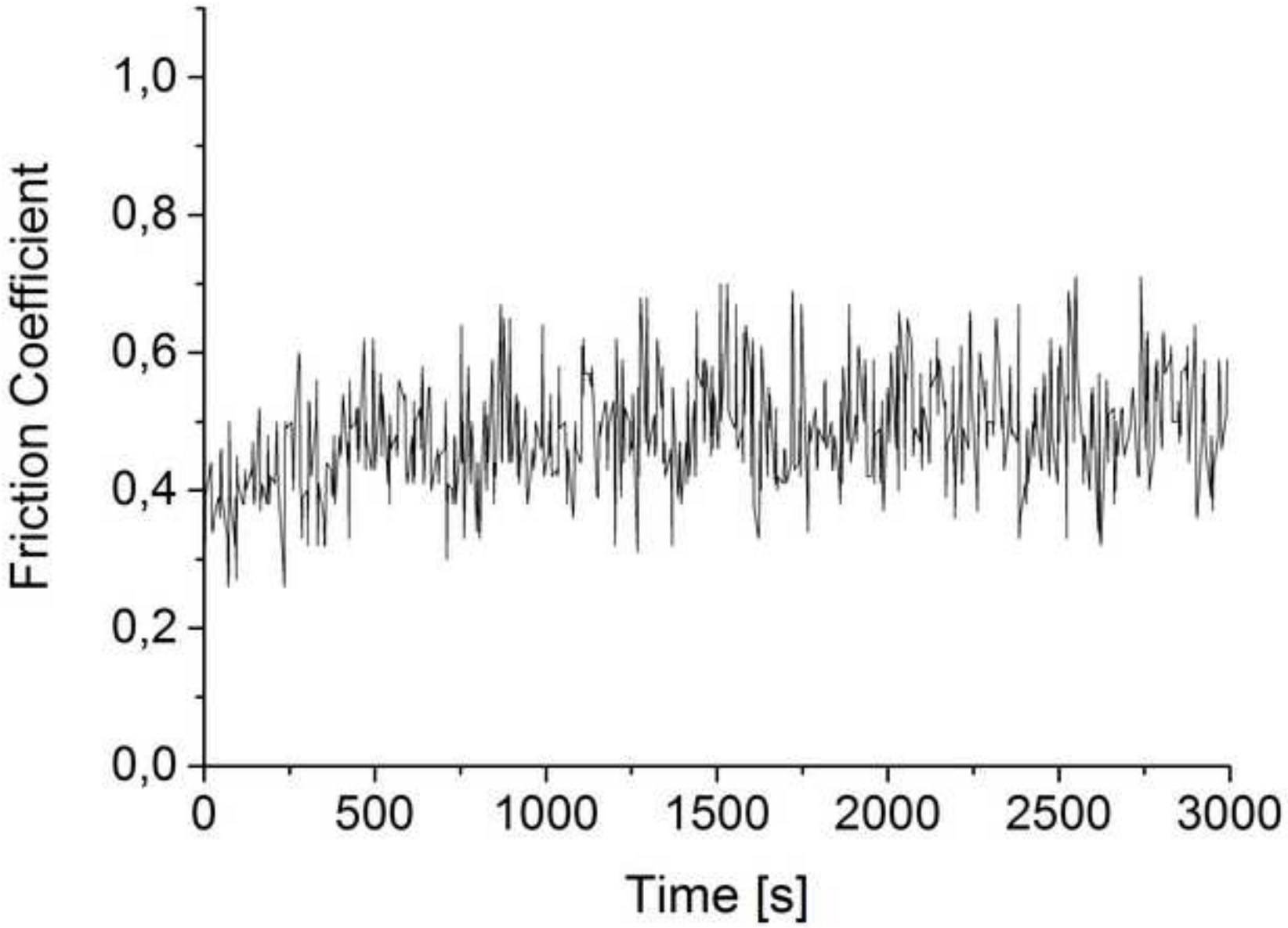

Figure 3b

Click here to download high resolution image

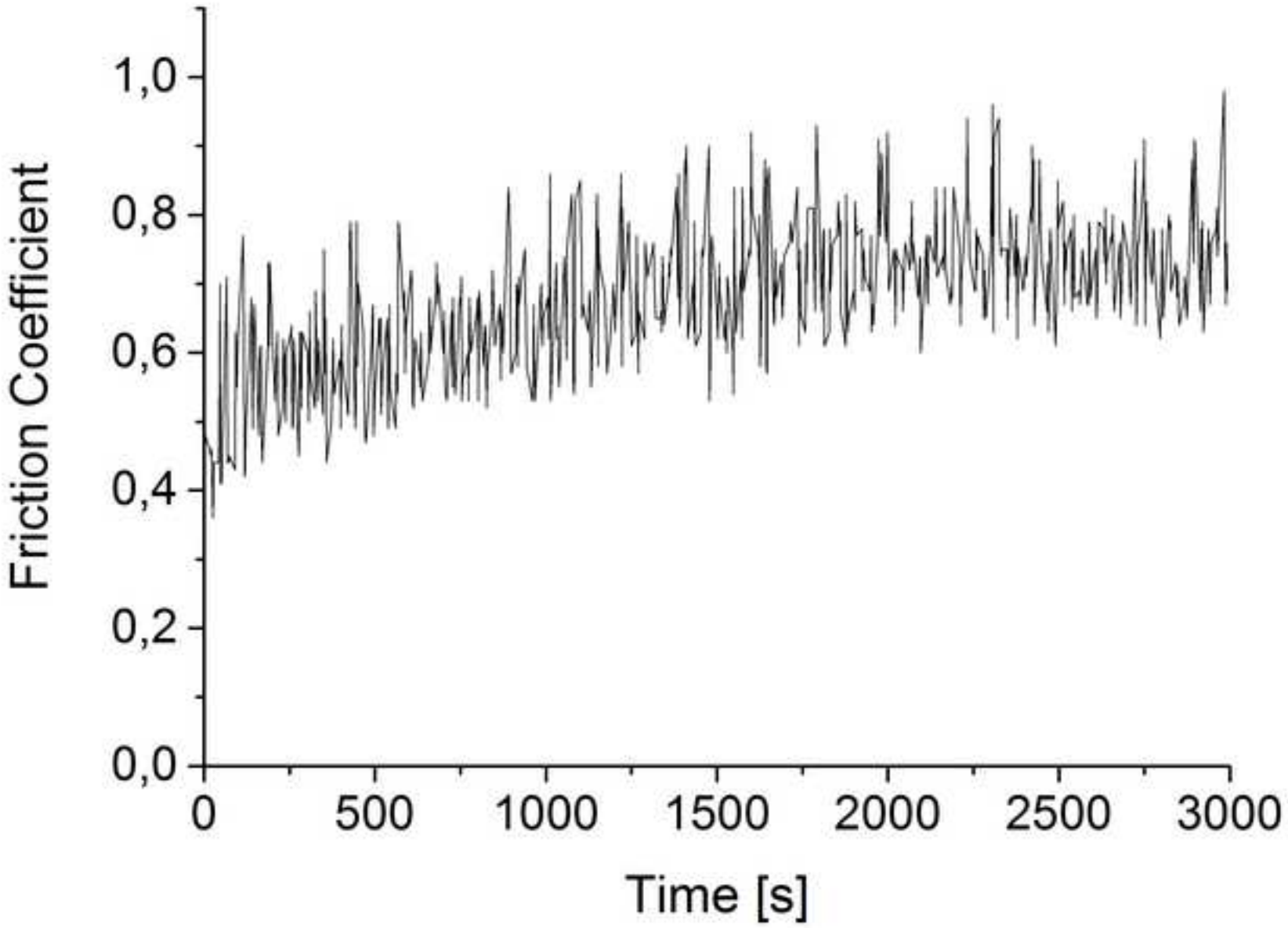

Figure 3c
Click here to download high resolution image

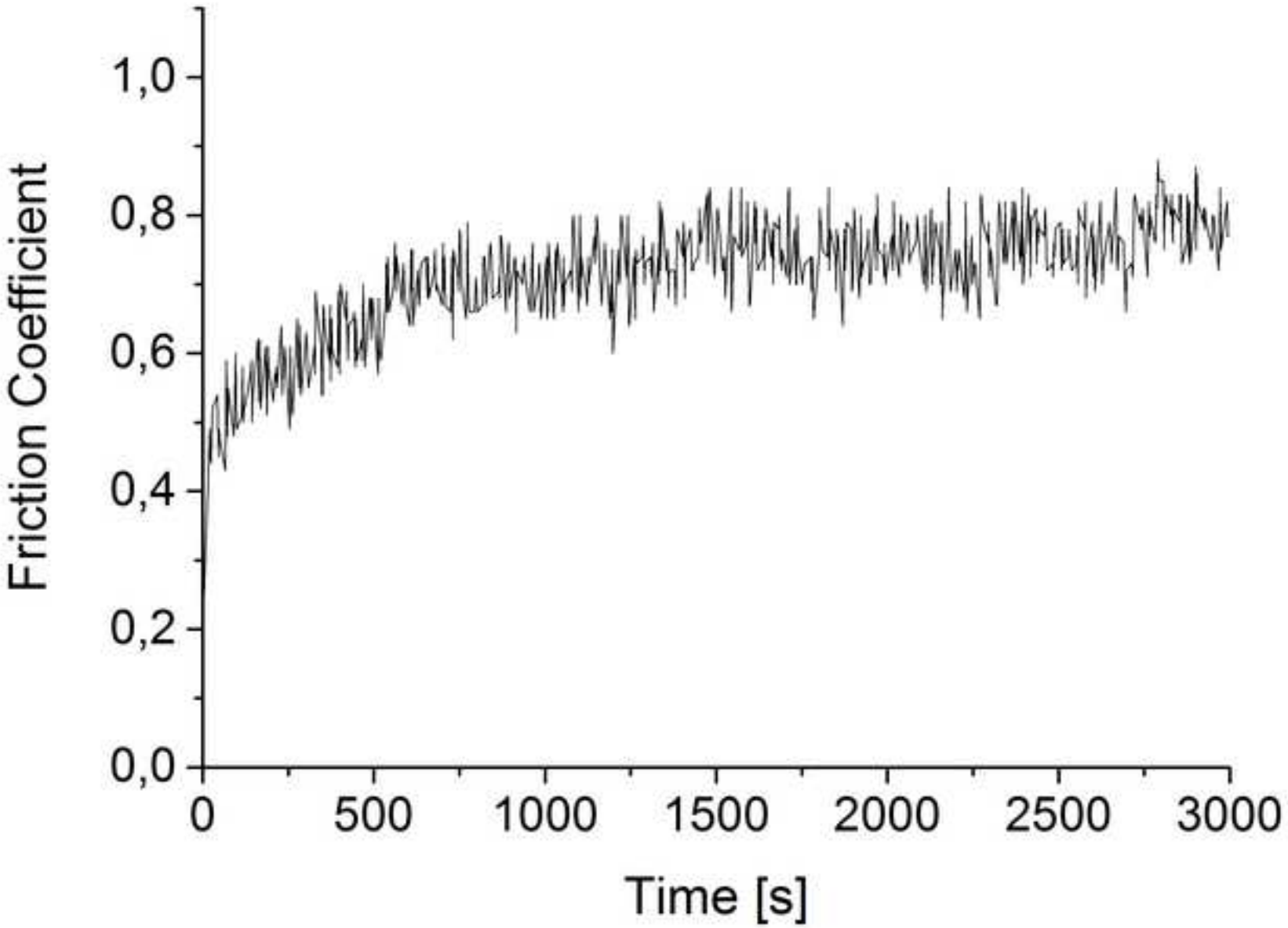

Figure 3d
Click here to download high resolution image

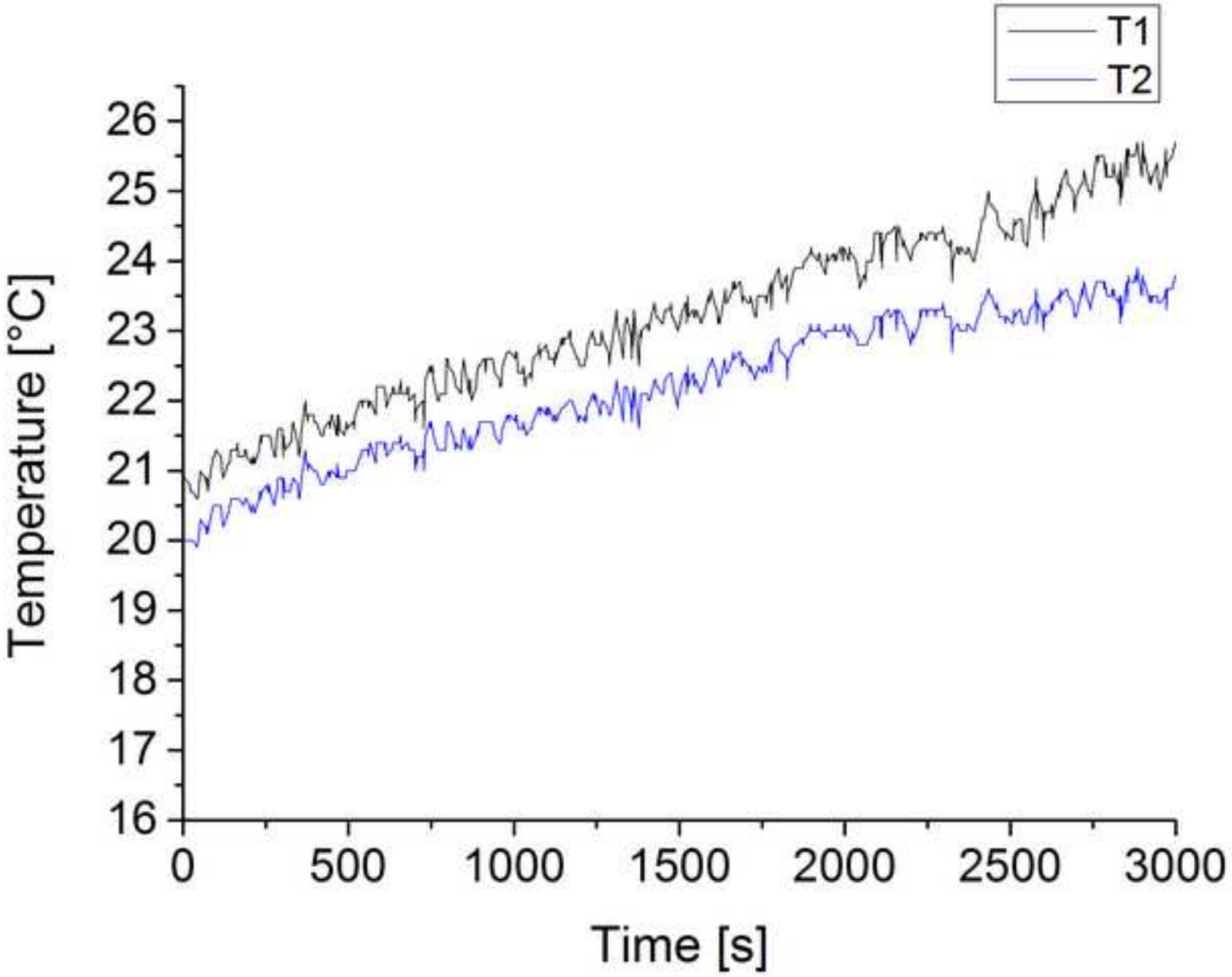

Figure 4a

Click here to download high resolution image

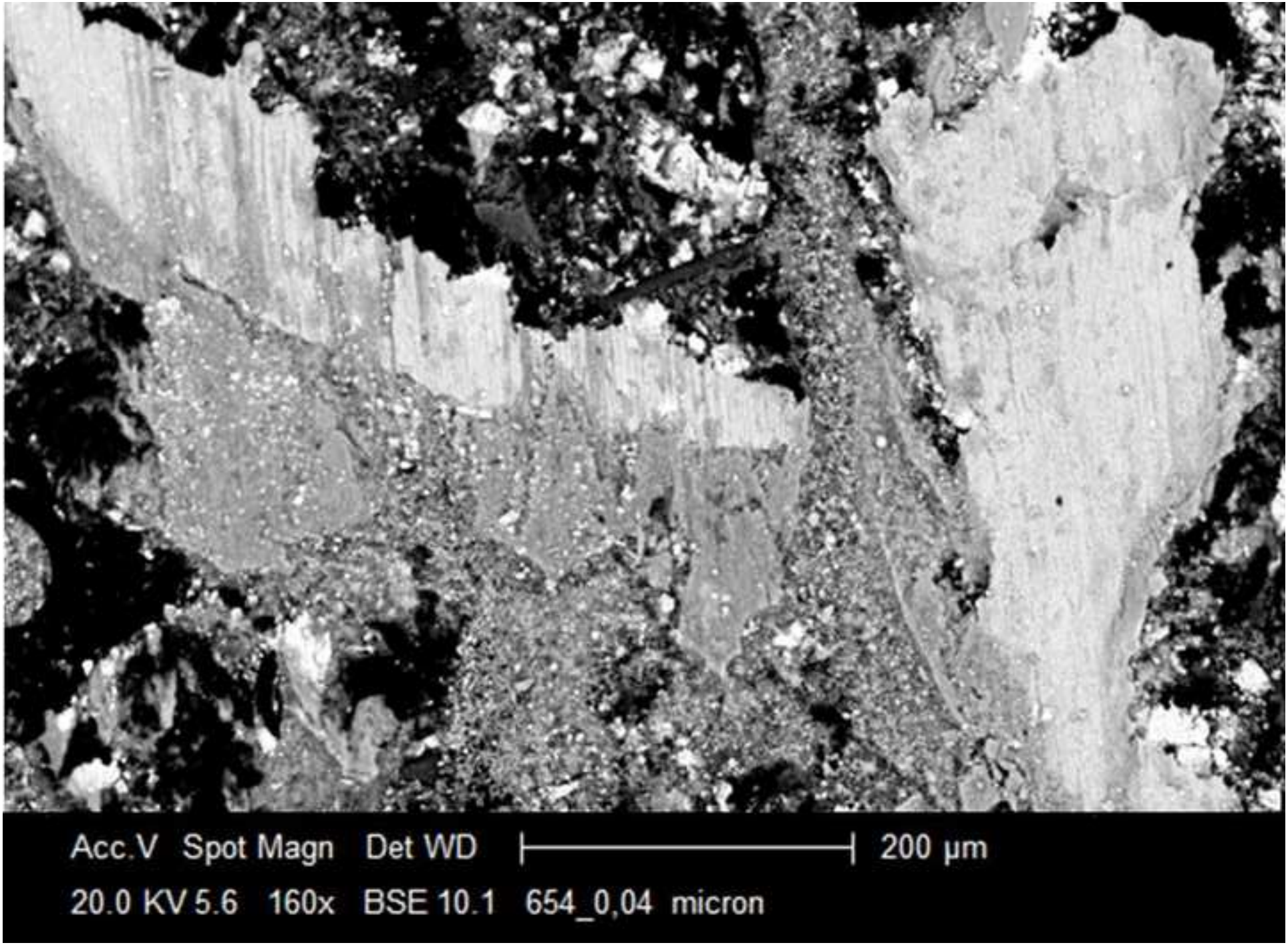

Figure 4b

Click here to download high resolution image

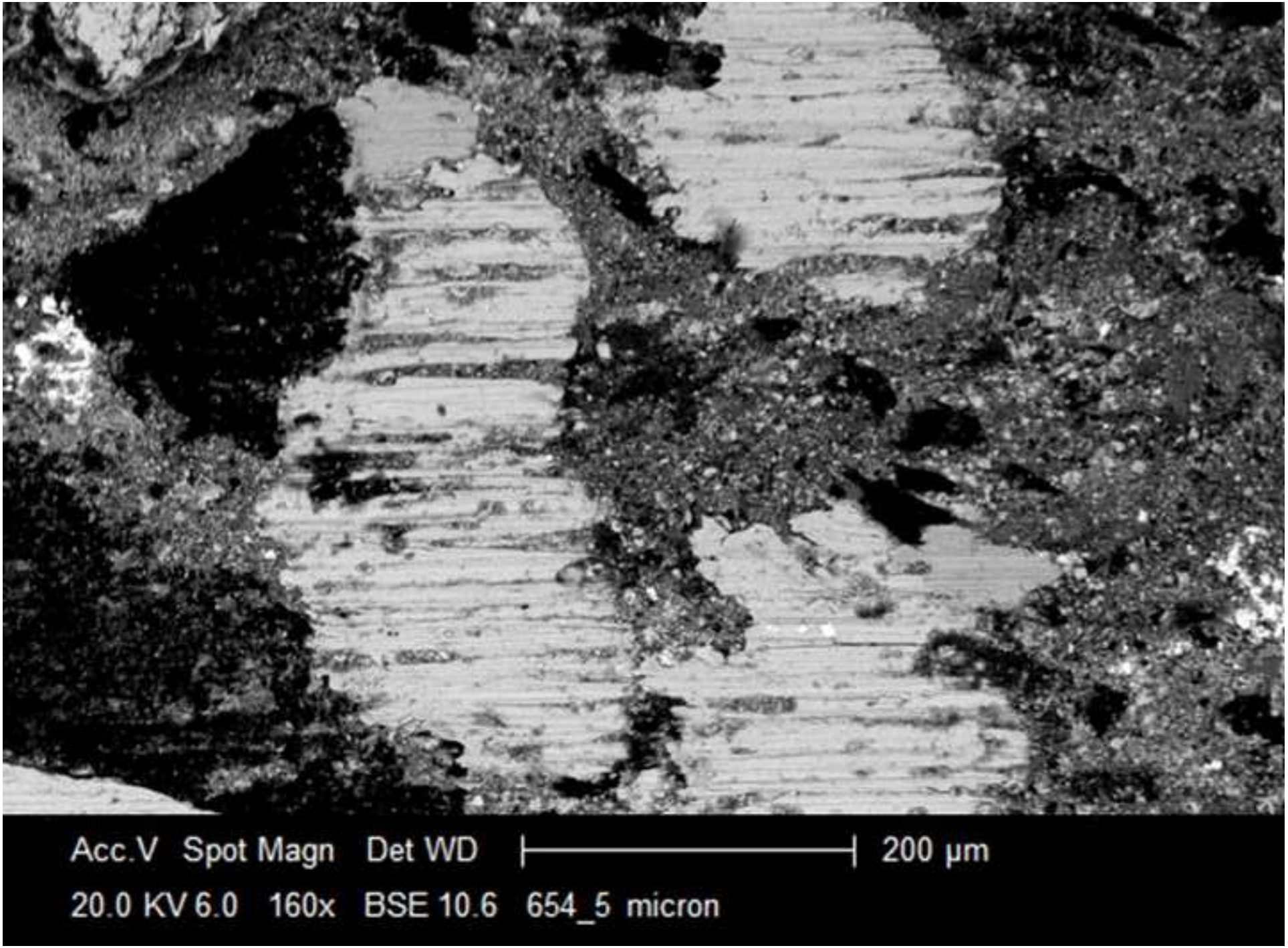

Figure 4c

Click here to download high resolution image

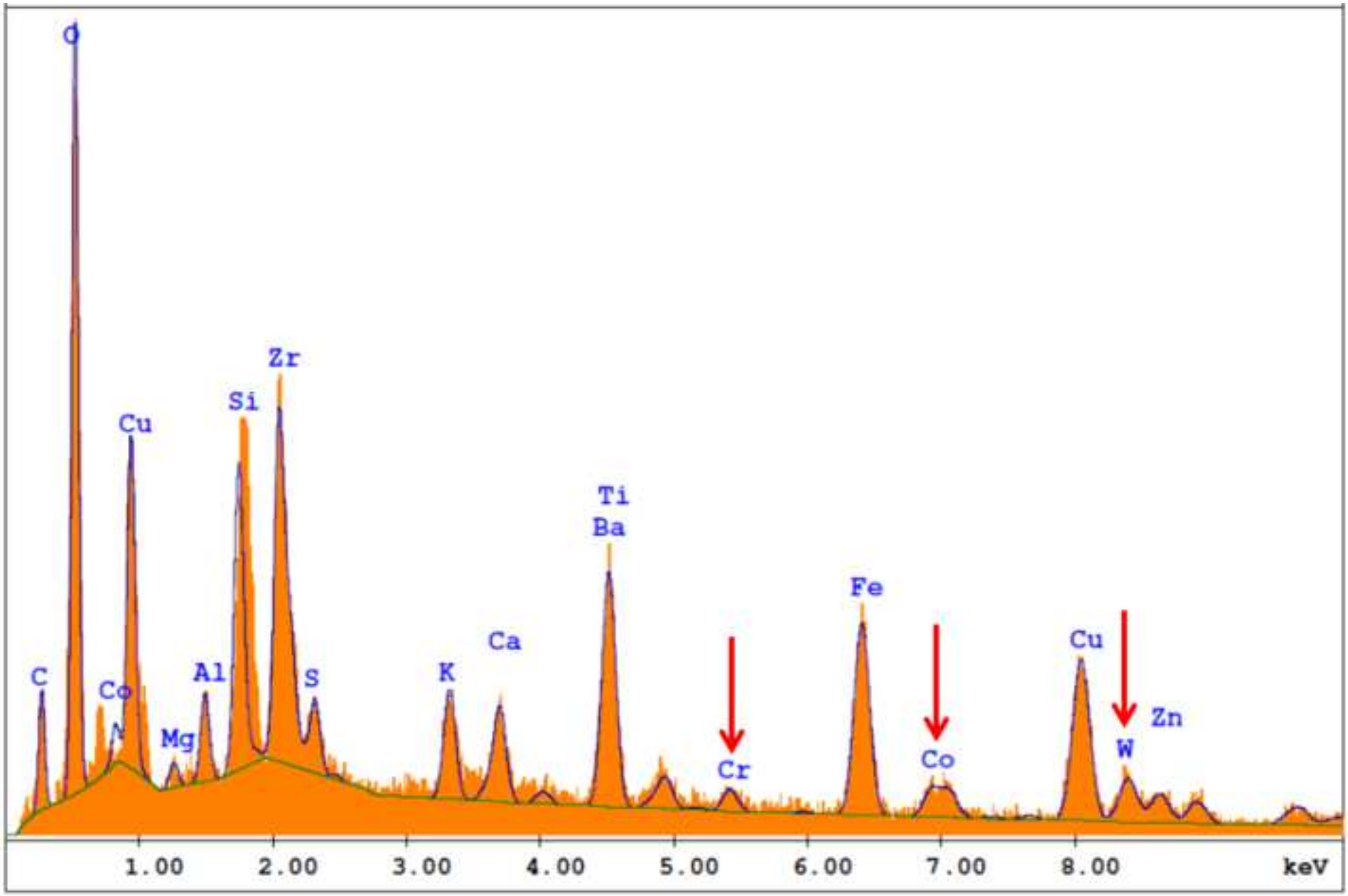

Figure 4d

Click here to download high resolution image

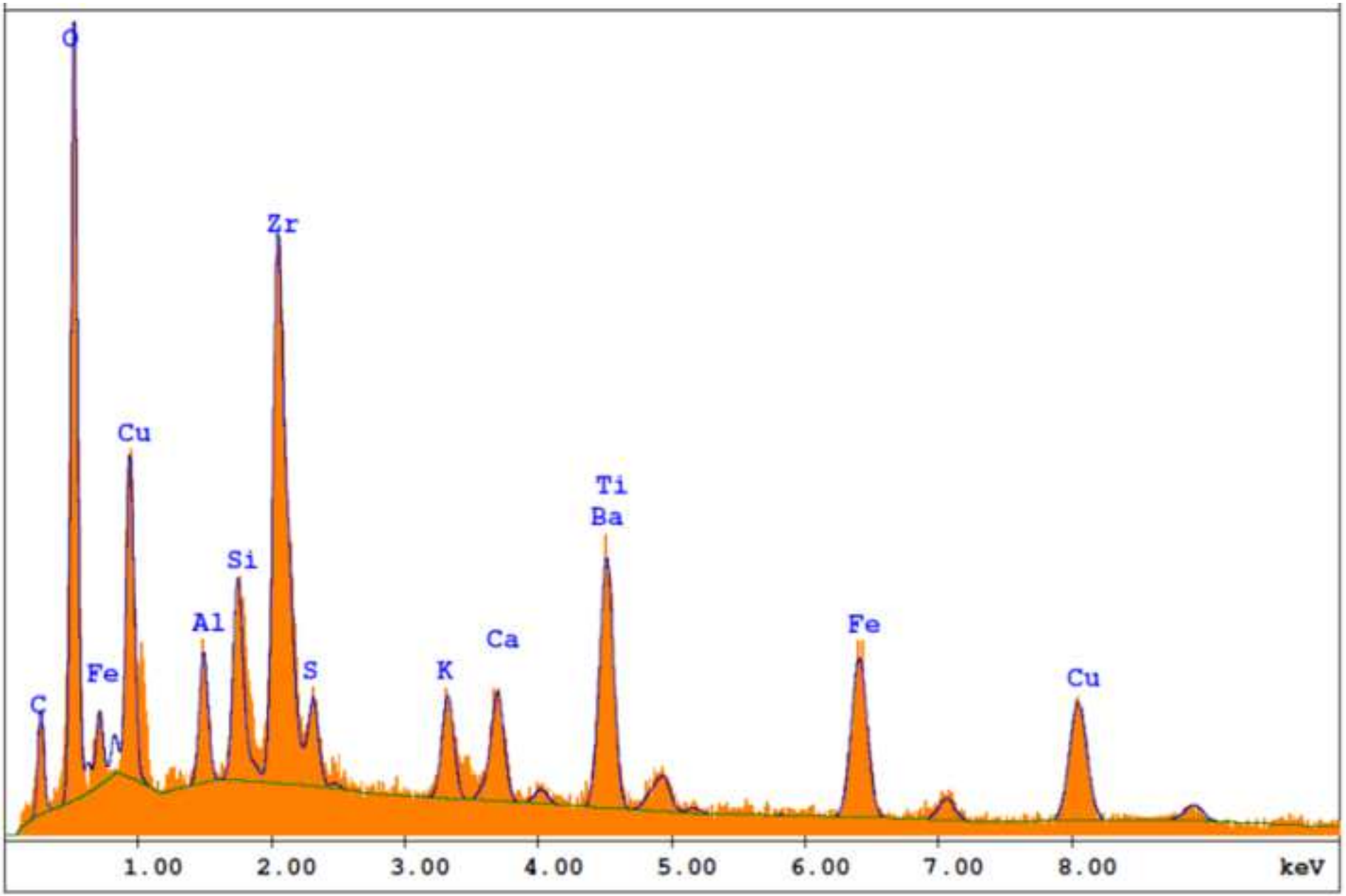

Figure 5a
Click here to download high resolution image

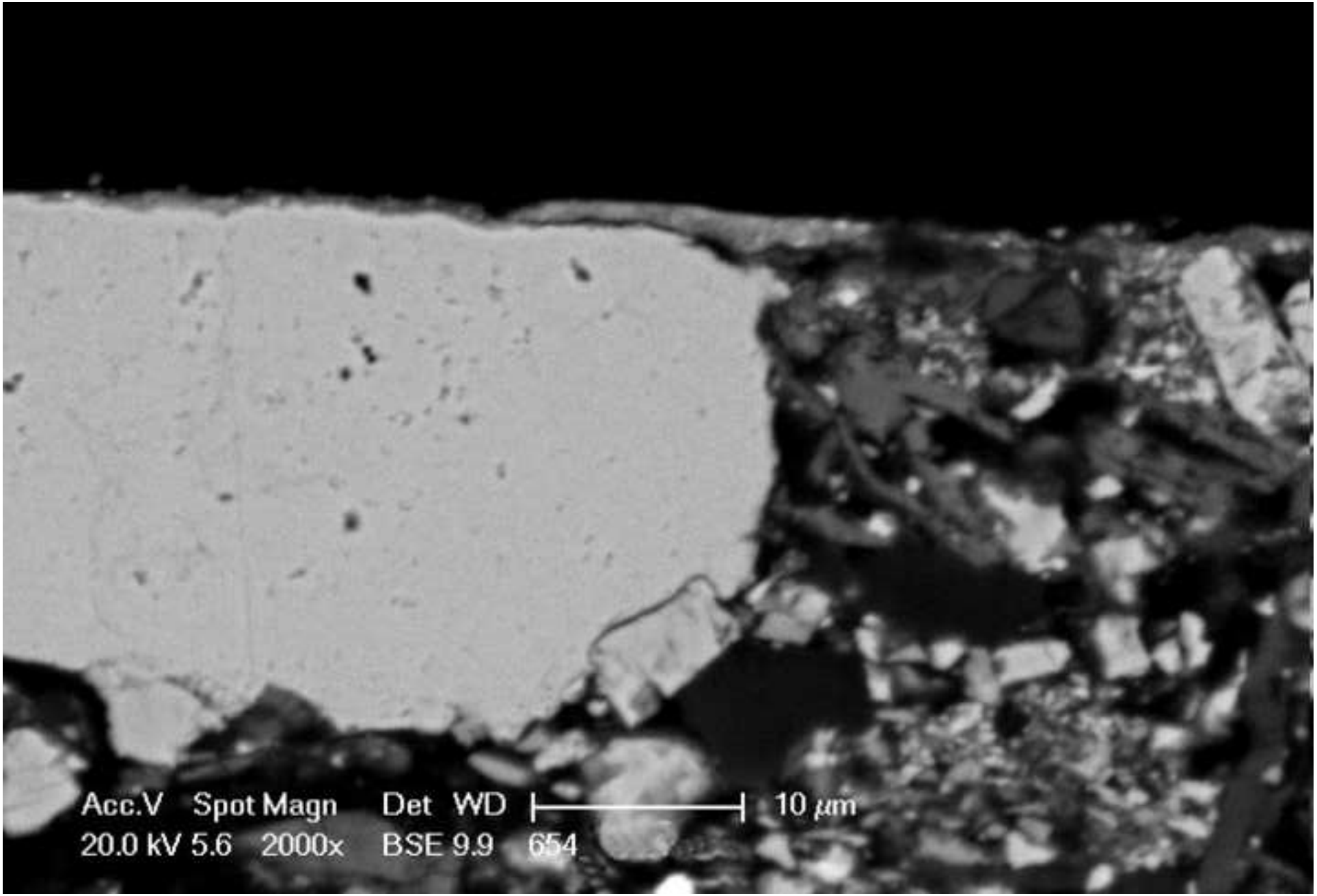

Figure 5b

Click here to download high resolution image

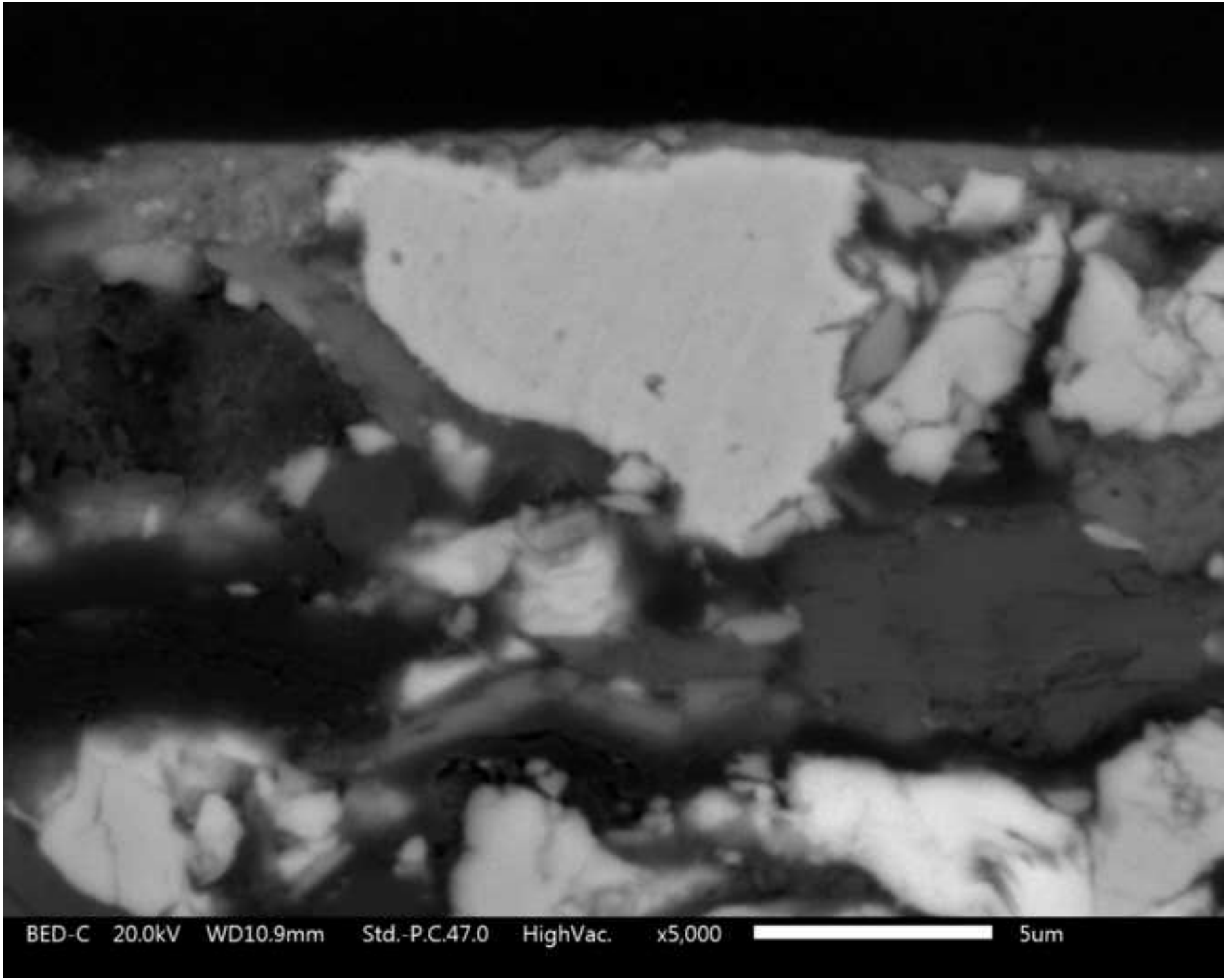

Figure 5c

Click here to download high resolution image

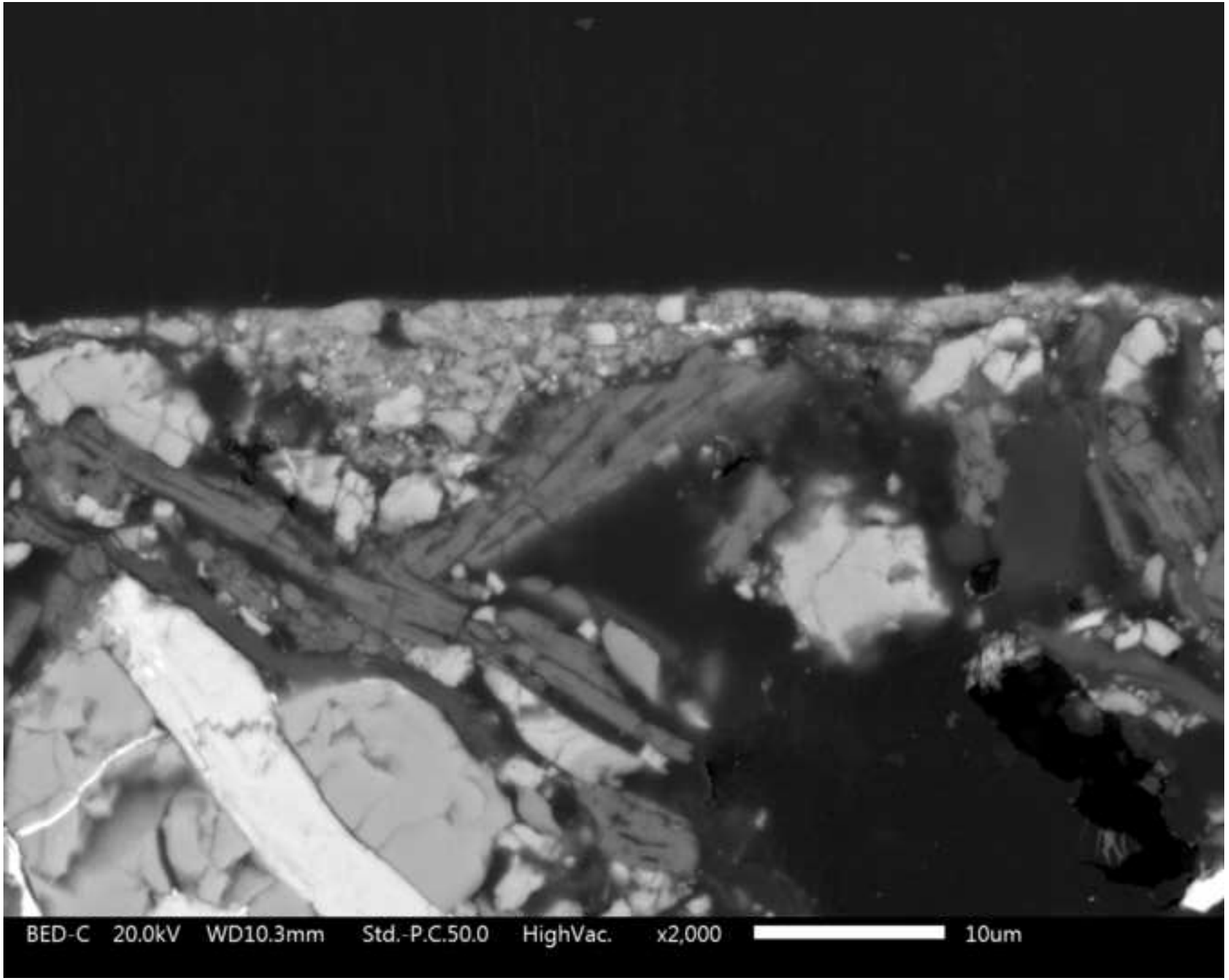

Figure 5d

Click here to download high resolution image

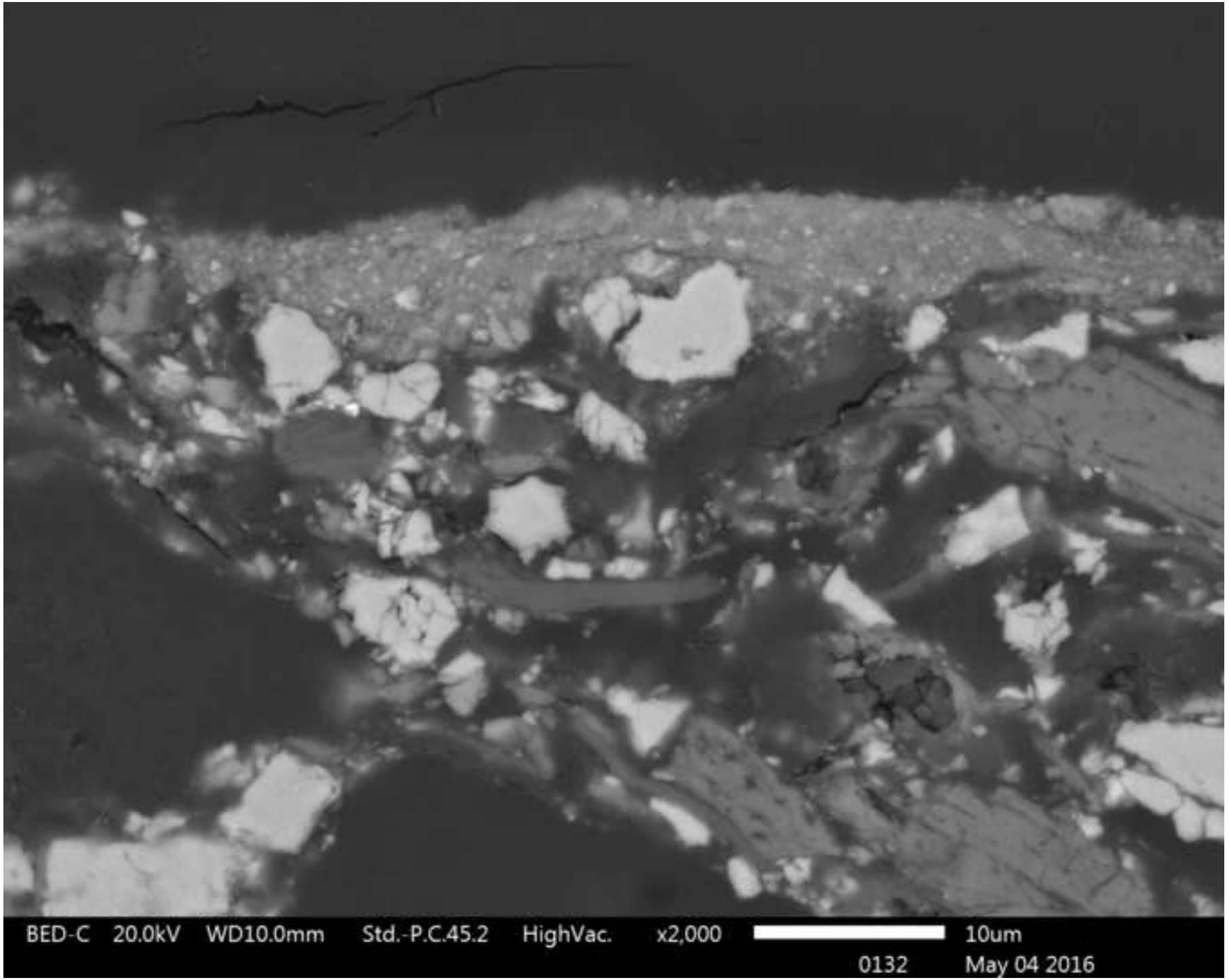

Figure 6a

Click here to download high resolution image

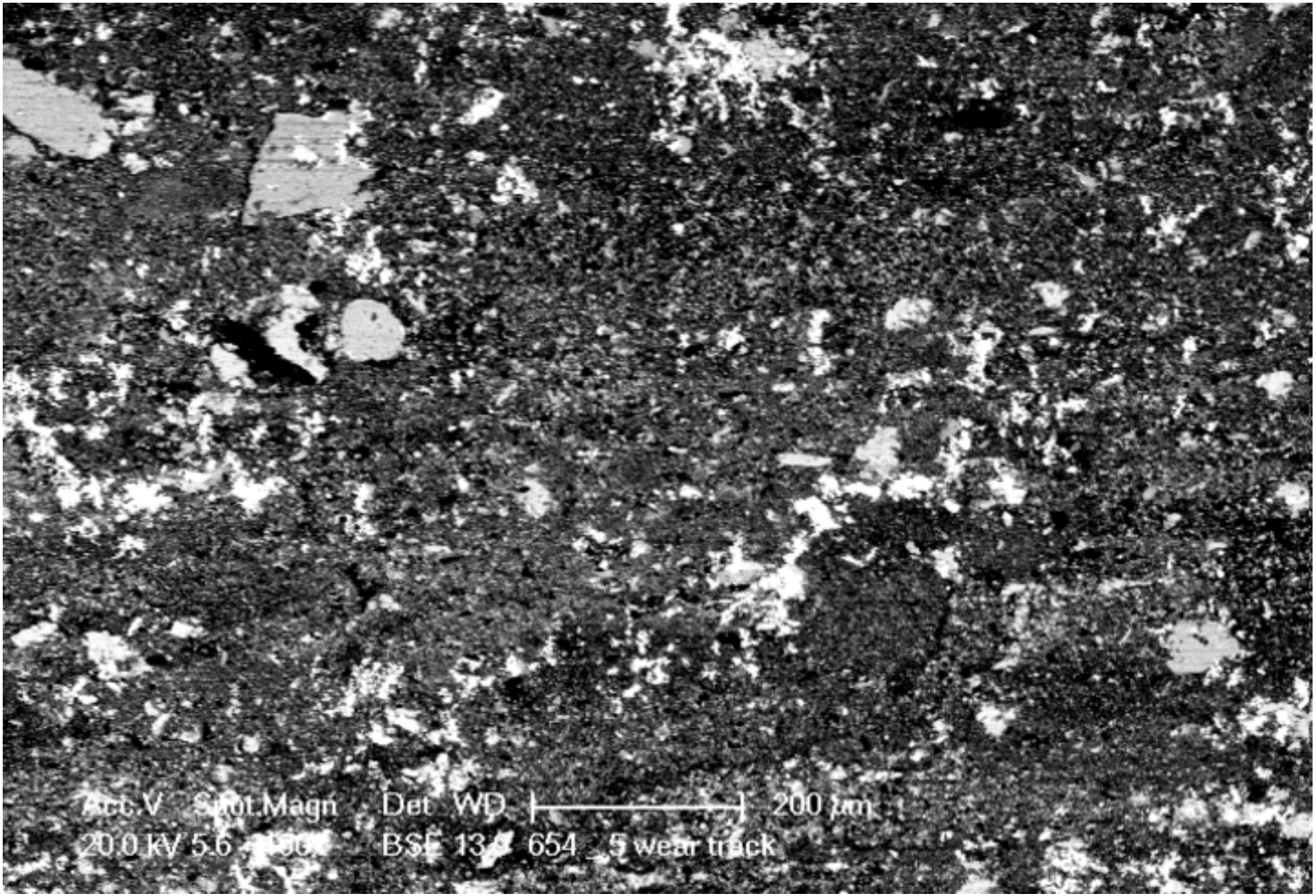

Figure 6b

Click here to download high resolution image

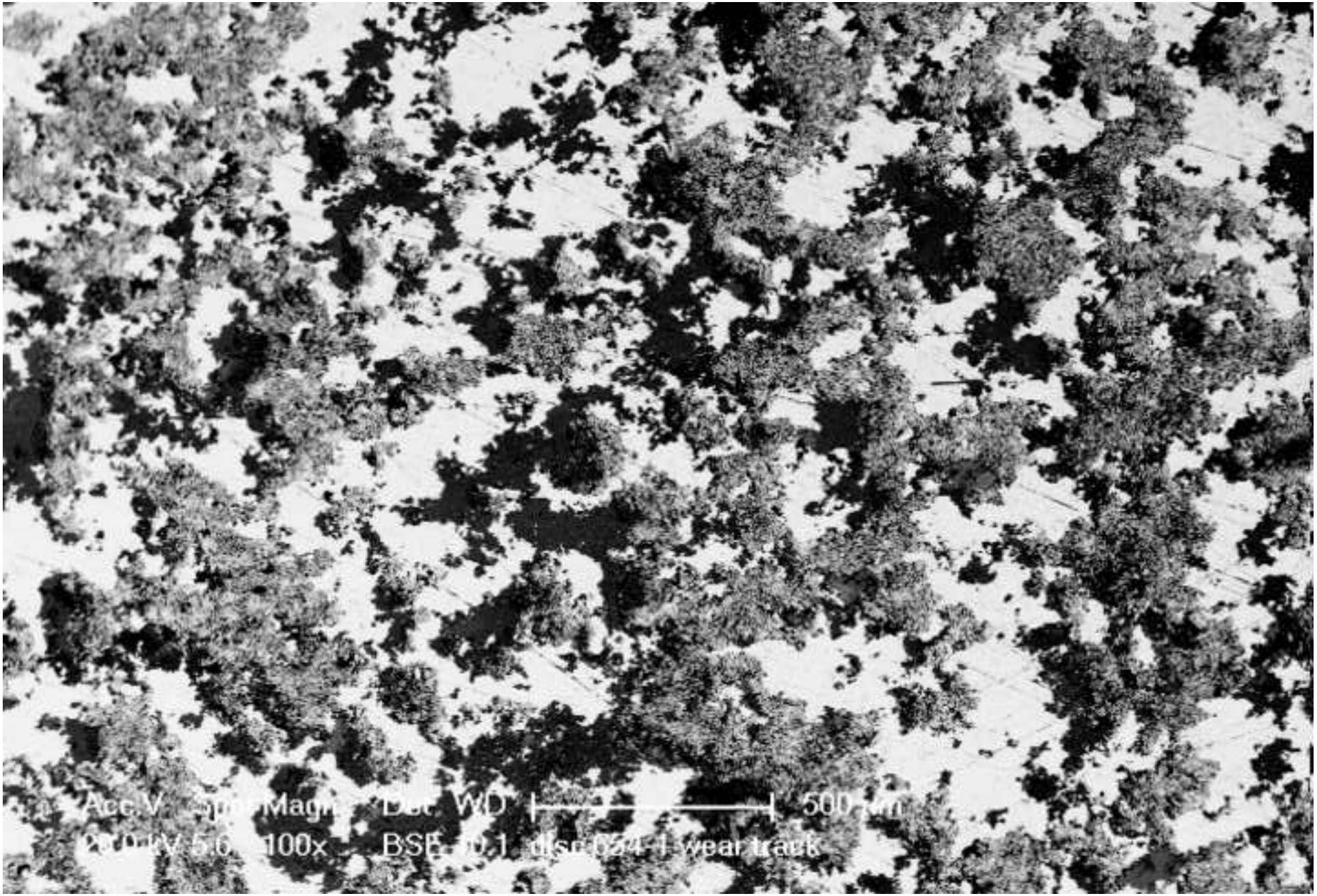

Figure 6c

Click here to download high resolution image

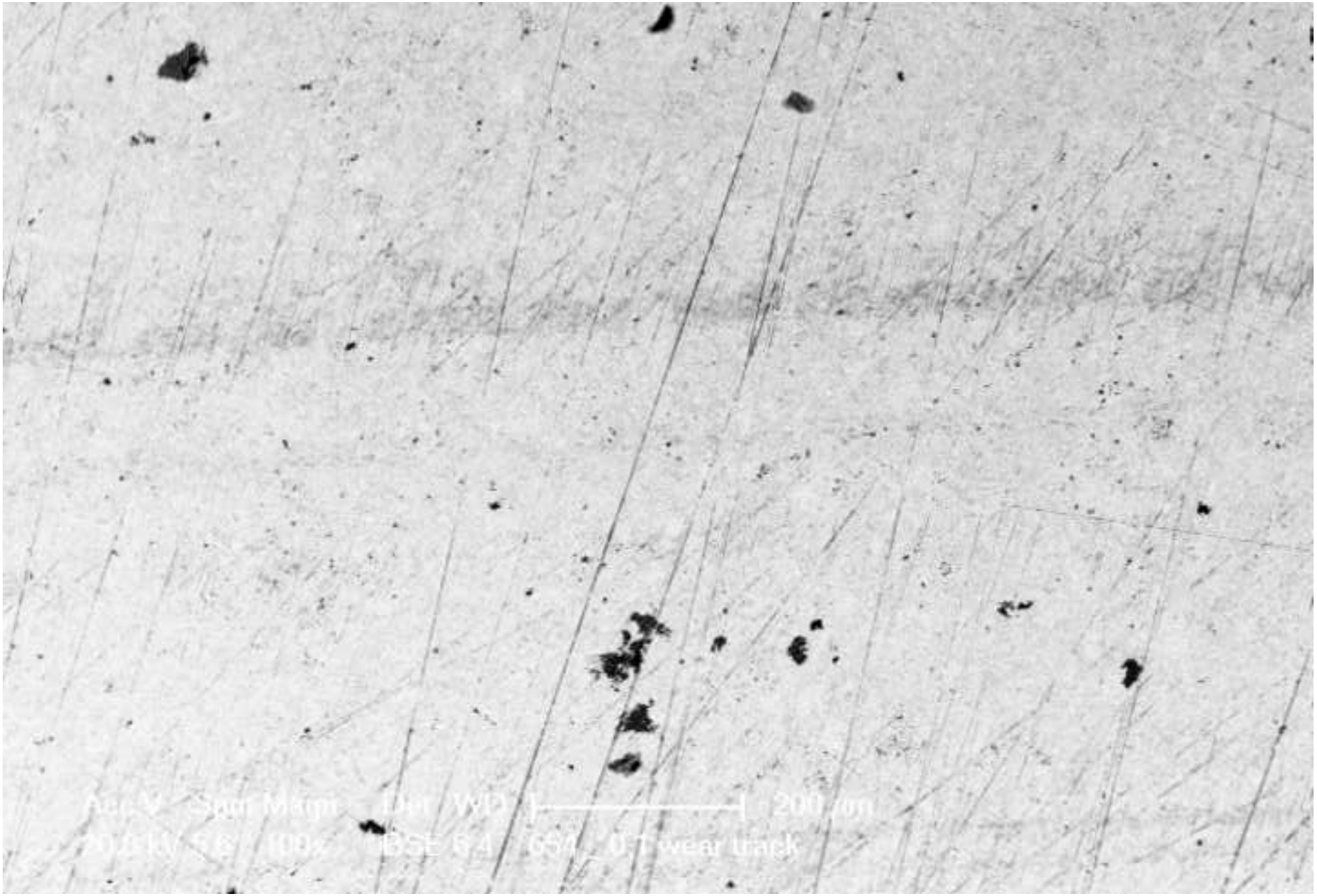

Figure 6d

Click here to download high resolution image

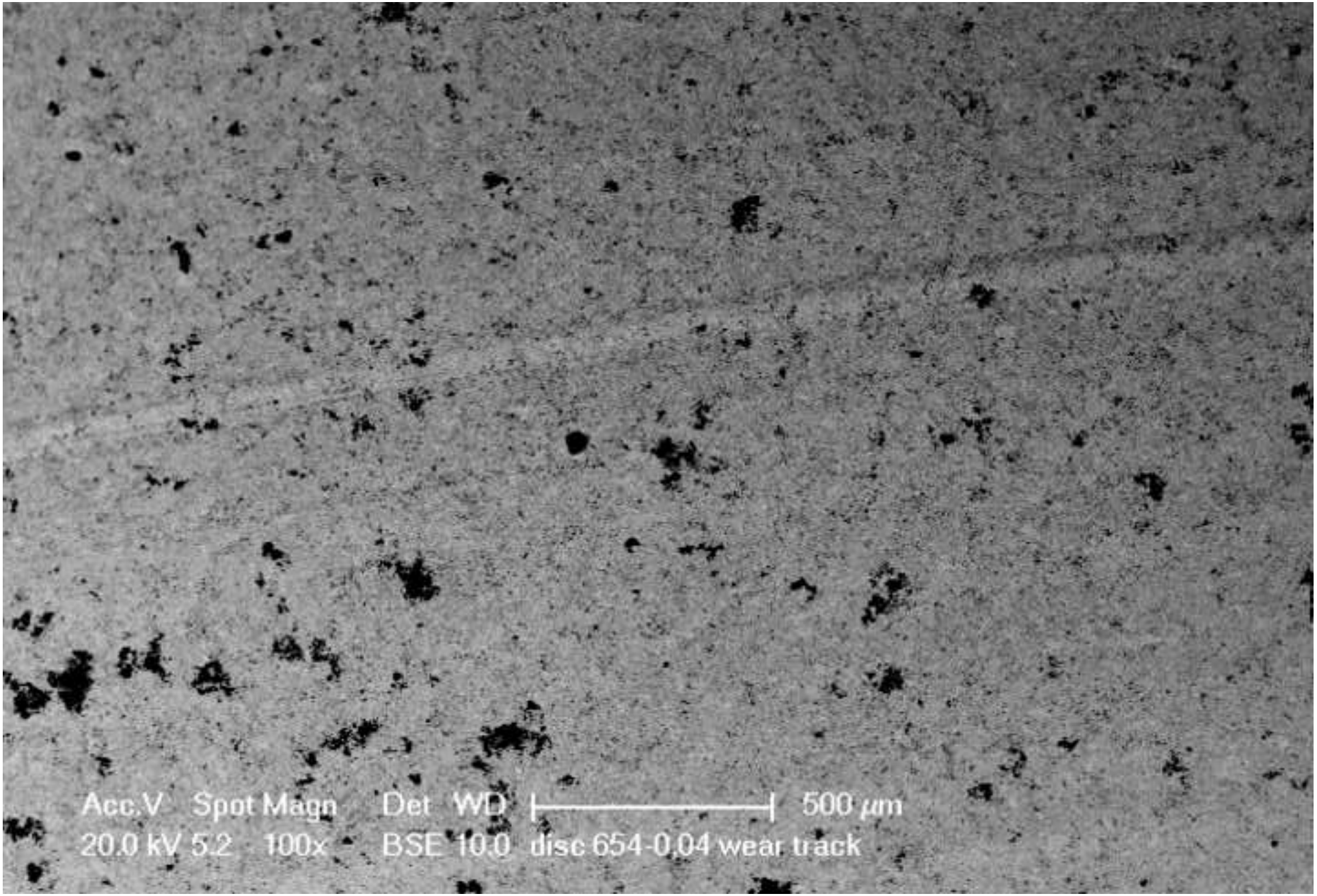

Figure 7a

Click here to download high resolution image

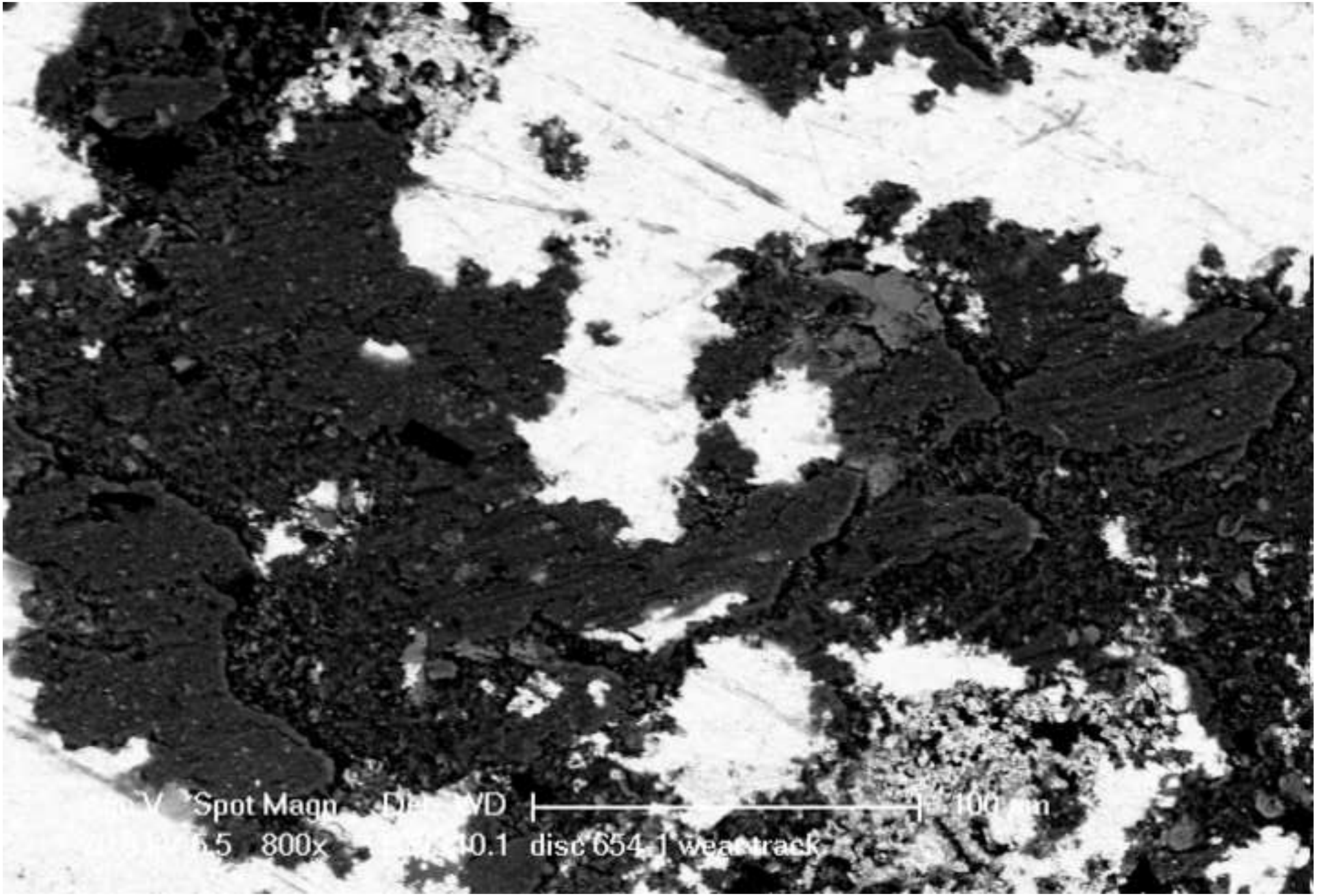

Figure 7b

Click here to download high resolution image

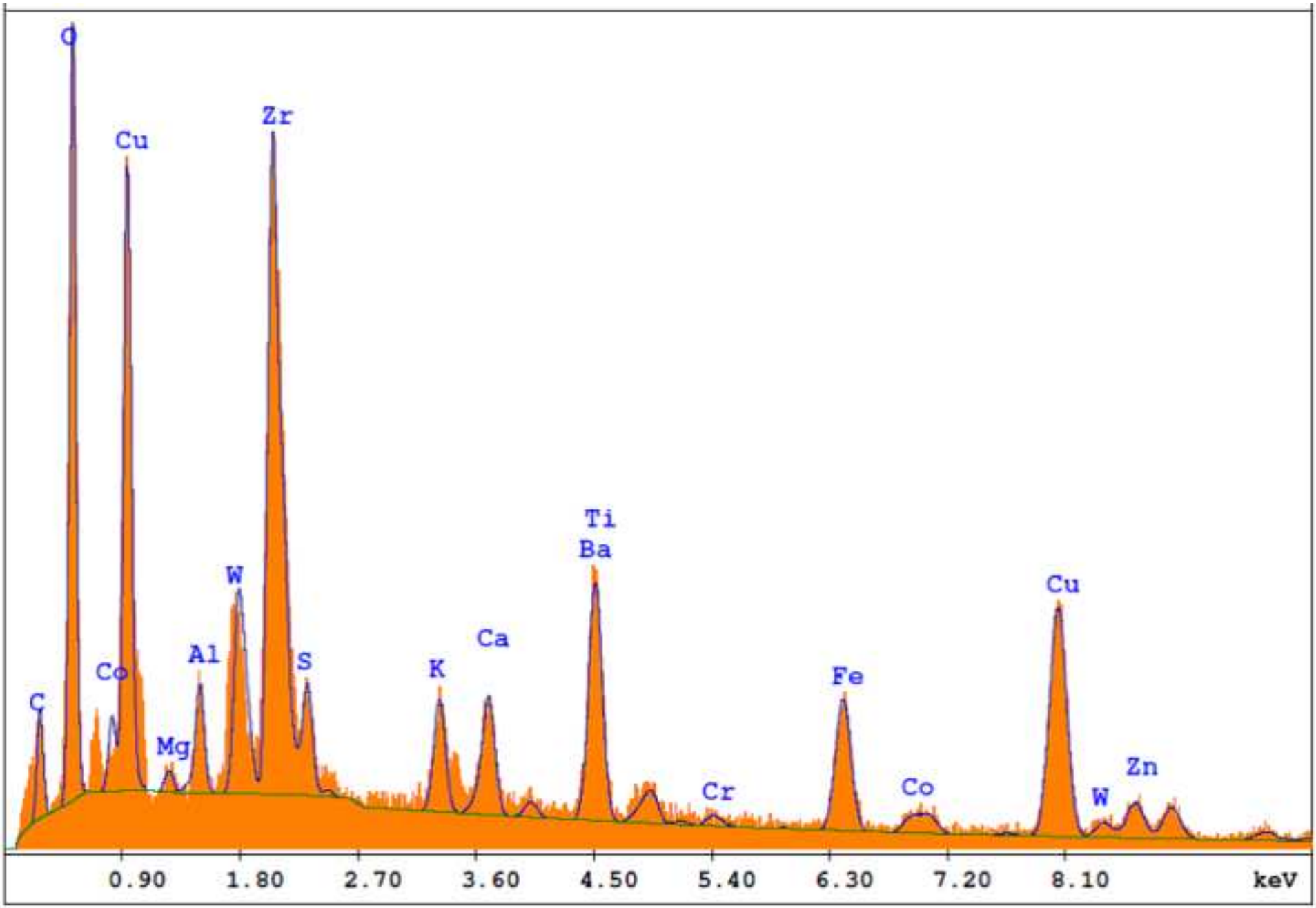

Figure 8

Click here to download high resolution image